Chapter 6

Study of parameters for PM monitoring in ambient air

The source origins exert a significant influence on the chemical composition and grain size distribution of atmospheric PM. Because PM from different sources exhibits different grain size distributions, there is no single parameter (such as PM10, PM2.5 or PM1) that is suitable for monitoring PM levels around all types of PM sources.

Campaigns for sampling and chemical characterisation of PM10, PM2.5 and TSP size segregated fractions and for measuring PM grain size distribution were performed in three types of environments in an attempt to assess the suitability of the different PM monitoring parameters around each source. The three selected areas were: a) the Barcelona Metropolitan Area - a typical urban environment where primary and secondary particles emissions occur, b) the surroundings of the Teruel power plant - an area where precursor emissions of secondary particles are quantitatively significant, and c) the ceramics production area of Castelló - an environment where anthropogenic primary particle emissions predominate.

6.1 PM characterisation in an urban environment

6.1.1 The study area

Barcelona and 32 surrounding towns make up the Metropolitan Area (604 km^2) with about 3 million inhabitants (half of the population of Catalonia, NE Spain). The urban development of this area forms a continuum along the Besòs and Llobregat rivers. One of the towns in this Metropolitan Area is L'Hospitalet de Llobregat, where the study site is located. This town has an important industrial area, with a total of 14207 companies, most of them related to services.

The urban dynamism around Barcelona accounts for a high road traffic density. According to the 1996 data supplied by the Metropolitan Transport Authority, the weekly mobility distribution in the Metropolitan Area of Barcelona is: 35.1% private cars, 31.1 % public transport, 33.8% pedestrian. The distribution of the journeys depending on the day of the week is as follows: 81.6% travel on week-days, 18.4 % at week ends. Furthermore, in addition to a wide range of industrial activities, two gas power stations (Besòs and Sant Adrià) and two city waste incinerators (Sant

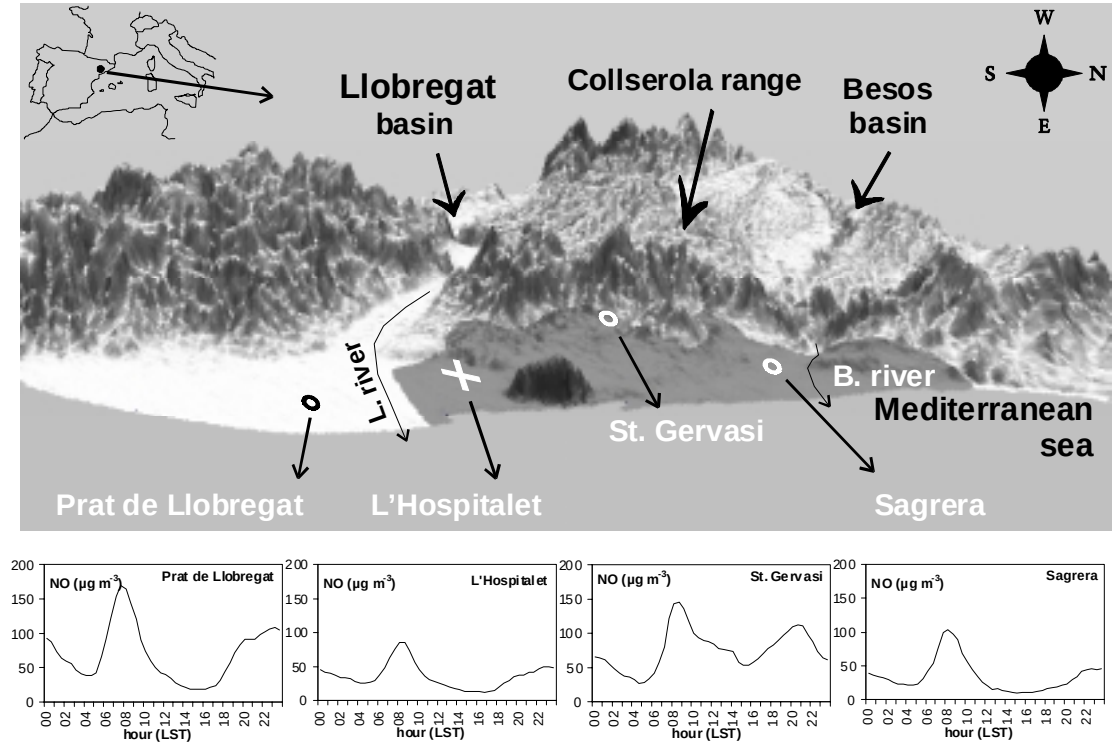

Figure 6-1. Location of the L'HOSPITALET and other (PRAT DE LLOBREGAT, St. GERVASI and SAGRERA) monitoring station in the Barcelona Metropolitan Area (shadow area) in North-eastern Spain and mean semi-hourly NO levels for the study period at these urban monitoring sites.

Adrià and Montcada) are also based in this area. Nevertheless, traffic constitutes the major source of air pollution in the area.

The orographic setting plays a key role in the atmospheric dynamics and therefore in the air quality of the Barcelona Metropolitan Area (Soriano et al., 1998 and 2001). The Metropolitan Area is located on the Barcelona coastal flat between the Mediterranean sea and the Collcerola range (525 masl) and between the basins of the Besòs (North) and Llobregat (South) rivers (Figure 6-1). This geographical context coupled with the prevalent meteorological scenarios accounts for the development of atmospheric circulations dominated by the sea breeze in summer and north winds in winter (Soriano et al., 1998).

In summer the anthropogenic emissions, mainly from traffic, reach a maximum from 8:00 to 11:00 h LST (local standard time) simultaneously with the development of an inland breeze flow (Toll and Baldasano, 2000). The industrial and urban areas of the Besòs and Llobregat basins emit pollution plumes which are transported inland towards the Vallés and Anoia depressions, where these external pollutants are mixed with significant local industrial and urban emissions. The Collcerola range also reinforces the breeze flow due to the anabatic winds. These inland fluxes over the southern Collcerola slope transport the contaminated air masses towards the top of the range. During this upwards transport the pollutants are injected at different atmospheric heights

by seaward flows prevalent at different altitudes in accordance with the time of day (Toll and Baldasano, 2000; Soriano et al., 2001). Consequently, some of these polluted layers injected at the lower atmospheric levels may reach the original emission source area in the afternoon.

In winter, low dispersive conditions due to nocturnal thermal inversion and a low breeze development account for the accumulation of local emissions in the coastal area during the morning (Soriano et al., 1998). In line with this scenario, in the mid morning, the breakdown of thermal inversion induces the dilution of the pollutants, even with emission rates being constant (Toll and Baldasano, 2000). When the thermal inversion breaks down, convective dynamic results in fumigation events giving rise to sporadic increases in levels of pollutants at the surface level. Finally, the thinning of the winter urban boundary layer accounts for a smooth nocturnal increase in levels of gaseous pollutants (with maximum concentrations recorded about midnight) at all the monitoring stations located in the Barcelona plain (Figure 6-1). The stations located at a given height over the sea level do not register this midnight increase in pollutants (St. GERVASI, Figure 6-1) probably, because they are outside the nocturnal mixing layer. High pollution events take place when inversion subsidence episodes are persistent in winter.

The daily cycle of levels of pollutants (Figure 6-1) is characterised by peak levels in the early morning followed by a noon decrease as a consequence of the dilution processes that are due to the thickening of the urban boundary layer. Furthermore, a midnight increase in pollutants is also evident in winter, which is probably due to the concentration processes caused by the thinning of the mixing layer (Allegrini et al., 1994).

In addition to the local PM emissions, Saharan dust outbreaks reach the Barcelona area at a mean rate of 7 to 10 events per year, with a major frequency in the summer and winter-spring periods.

6.1.2 Sampling and measurements

The traffic/urban air quality monitoring station of L'HOSPITALET (located at Avenue Torrent Gornal, in Barcelona Metropolitan Area, Figure 6-1) was selected for PM10 and PM2.5 continuous measurement and sampling. Continuous measurements of PM grain size distribution were performed with a GRIMM 1108 (Labortechnik GmbH & Co. KG) laser spectrometer. This dust monitor determines the particulate matter levels in 15 different grain-size channels from 0.3 to >20 µm. PM10 GRIMM levels were compared throughout the study period with gravimetric measurements to check the data set quality (Figure 6-2).

The sampling of TSP grain-size fractions (7 stages from 0.3 to >20µm) was performed by means of a Retsch PI-1 cascade impactor, whereas PM10 and PM2.5 was sampled with high vl. Sampler following the methodology described in chapter3. Once the levels of bulk particulates were obtained by weighting the filters using standard procedures, levels of major and trace chemical species were determined in the filters and cascade impactor samples following the procedures described in chapter 3. A total of 7 cascade impactor samples distributed throughout the different seasons were taken from June 1999 to June 2000.

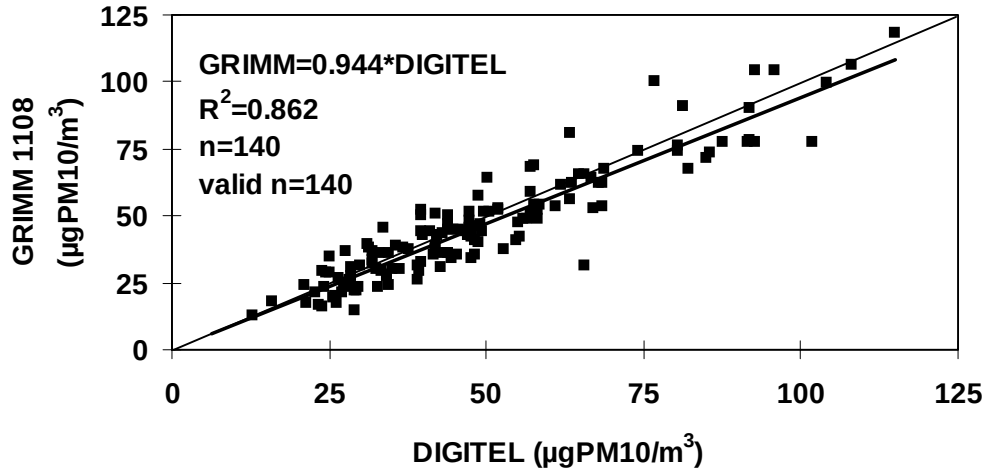

Figure 6-2. Comparison of the daily PM10 levels obtained with the laser spectrometer and with the DIGITEL PM10 high volume sampler.

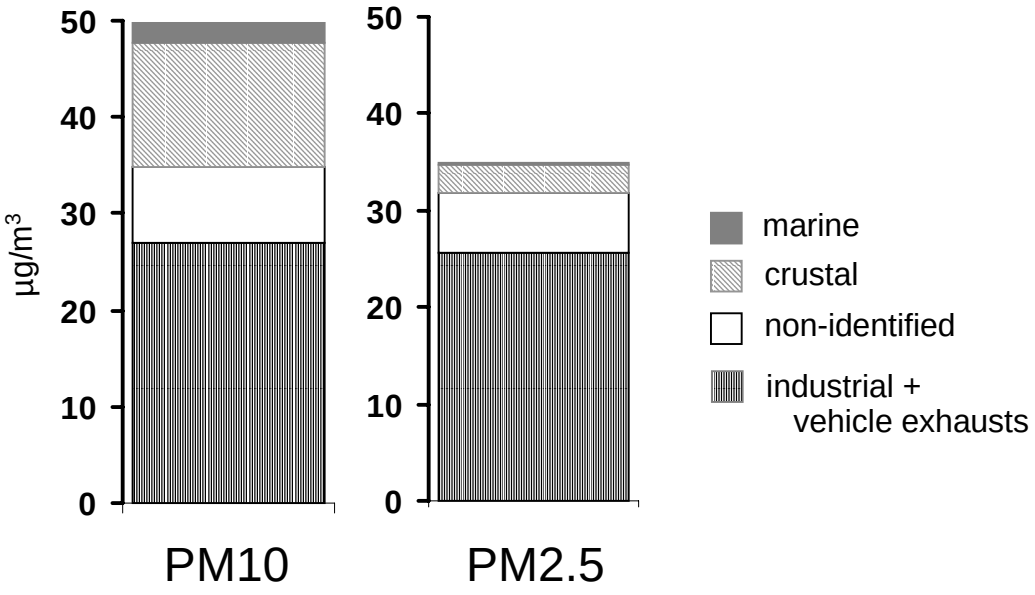

Figure 6-3. Mean PM10 and PM2.5 source contribution at L'HOSPITALET station (Barcelona Metropolitan Area; marine = Na+Cl+ss-$SO_4^=$; crustal = Al_2O_3, SiO_2, $CaCO_3$…; industrial + vehicles exhaust = nss-$SO_4^=$+NO_3^-+NH_4^++OC+EC….; non-identified = difference between gravimetric and chemically determined PM10 level).

Levels of NO, NO_2, CO, O_3 and SO_2 were also monitored by means of standard methods. This site was selected because it is representative of the stations in the Barcelona Metropolitan Area (and in the whole of Spain), which are located at kerbsides.

6.1.3 PM10 & PM2.5 ambient levels

Mean PM10 and PM2.5 levels recorded at L'HOSPITALET in the study period reached 40.6 μgPM10/m^3 and 27.7 μgPM2.5/m^3 with 98 % of daily data coverage. These values are very high when compared with the PM10 annual and 24-hour limit values of the new EU Air Quality Directive. However, it should be noted that this is a kerbside. Mean annual levels of TSP and PM1 reached 59 and 19 μg/m^3, respectively. The mean PM10 and PM2.5 levels calculated from this set of continuous measurements are slight lower than the mean annual levels (by 24%) calculated from the gravimetry set of measurements (presented in Figure 6-3 and chapter 5) due to the exclusion of weekend sampling in the gravimetric sampling, when PM levels usually decrease. As stated in chapter 5, where the PM10 and PM2.5 chemical characterisation and the source apportionment at L'HOSPITALET were presented, PM derived from industrial and vehicle exhaust emissions mainly occurs in PM2.5 whereas crustal PM and sea spray mainly occur in the 2.5-10μm fraction (Figure 6-3).

TSP, PM10, PM2.5 and PM1 were higher in autumn and winter (Figure 6-4), when frequent high PM events were recorded. This seasonal trend is parallel to that recorded for NOx levels, and consequently local emissions are expected to control the PM levels. However, since PM levels are still high in August and March, when levels of gaseous pollutants decrease drastically, external PM inputs may be expected in these periods.

As at most kerbsides, the daily trend of hourly TSP and PM10 levels (Figure 6-5) reflects the road traffic flow, with maximal levels in the rush hour (7:00-11:00 and 18:00-21:00 h LST periods). However, the hourly PM2.5 and PM1 levels only reflect the morning traffic emissions. The evening PM10 peak is more evident in winter and autumn than in spring and summer. Furthermore, PM10, PM2.5 and PM1 levels (for the whole year, but especially in winter) tend to increase slightly from late afternoon to midnight (Figure 6-5). This trend is similar to the hourly evolution of gaseous pollutants and also shows a secondary midnight increase (Figures 6-1, 6-4 and 6-14) at all the monitoring stations on the Barcelona coastal plain. This has been attributed to the nocturnal concentration of pollutants due to the thinning of the urban boundary layer (Allegrini et al., 1994).

NO, CO, PM1 and PM2.5 levels are considerably higher in winter than in the other seasons (Figure 6-4). However, PM10 and TSP levels are very close for all the seasons in the period 0:00 to 12:00 h LST (+2 and +1 h GMT in winter and summer, respectively), but much higher in the period 13:00 to 23:00 h LST in autumn and winter (Figure 6-5). These higher levels of coarse particles recorded in the afternoon and evening of the colder seasons are probably the consequence of the lower winter dispersive conditions.

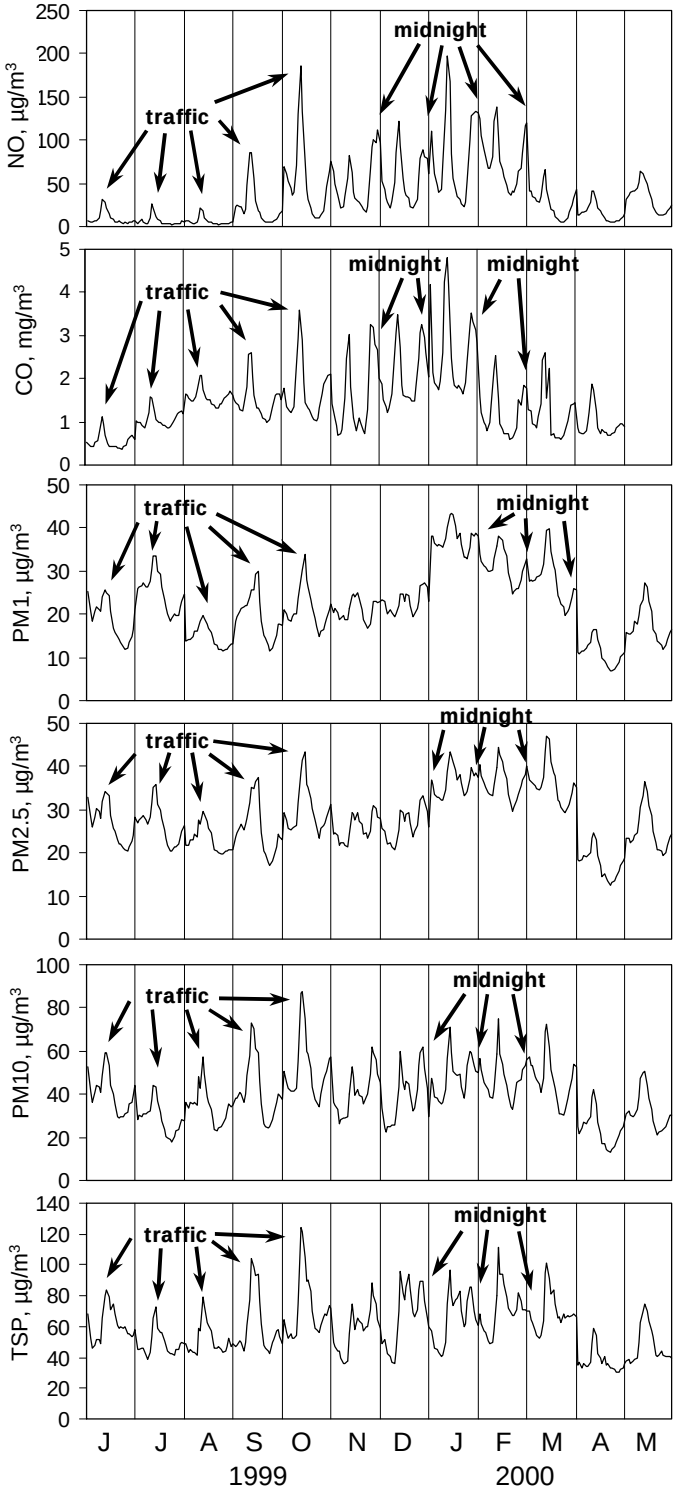

Figure 6-4. Monthly NO, CO, PM1, PM2.5, PM10 and TSP levels recorded at L'HOSPITALET from June 1999 to May 2000.

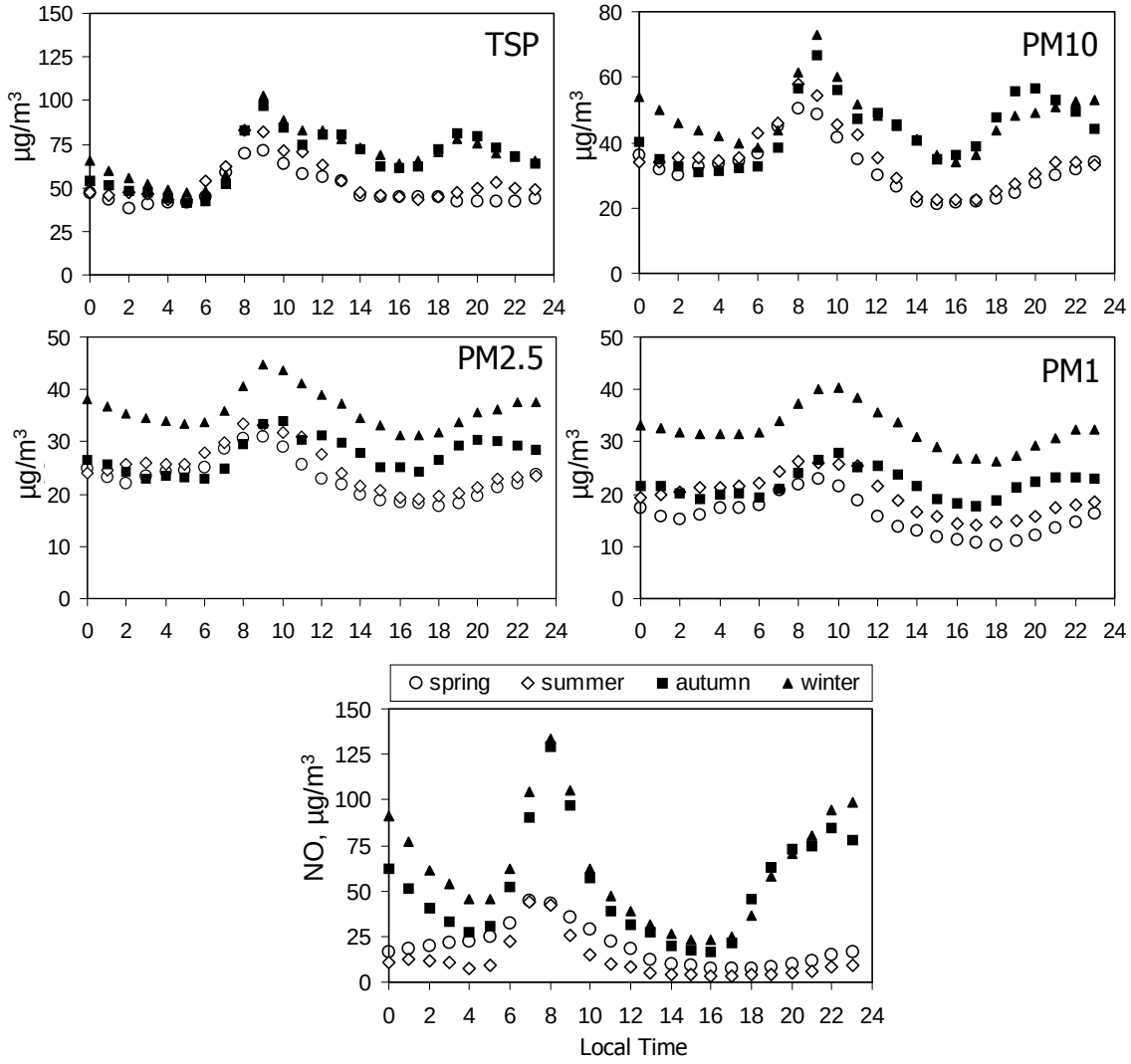

Figure 6-5. Seasonal variation of the hourly TSP, PM10, PM2.5, PM1 and NO levels recorded at L'HOSPITALET from June 1999 to May 2000.

6.1.4 Cascade impactor sampling

Seven cascade impactor samples were taken throughout the different seasons from April 1999 to June 2000 in order to characterise the grain size distribution of PM species. The analysis of the water soluble species was performed in the 7 samples. Levels of the non-water soluble (insoluble) species were also determined in 4 samples, whereas the carbon content was determined in 2 samples. The results are shown in Figures 6-6 to 6-12.

Ti, Al, Cr, Fe, Cu, Pb, V and Ni are mainly present in the insoluble fraction (99% of Ti, 95% Al, 72% Fe, 66% Cu, 64% Pb, 63% V, 38 % Ni). Mg, K, and Mn are significantly present in both soluble and insoluble fractions (41% Mg, 48% K and 64% Mn in the soluble phase). Sr, Ca, Zn, Na, $SO_4^{=}$, NO_3^{-} and NH_4^{+} are mainly present in the soluble fraction (74% of Sr, 80% of Ca and Zn, and >95% of $SO_4^{=}$, NO_3^{-} and NH_4^{+}).

Sulphate is mainly present in the finest fractions (<1.5µm) of PM. Around 66% and 55% of sulphate-mass is present in the PM fractions <3.0 and <1.5µm, respectively, on average. Ionic balance analysis indicates that the load of ammonium-sulphate accounts for 50-70% of total sulphate in most of samples, the remaining 50-30% occurring as calcium-sulphate. The maximum and minimum proportions of ammonium-sulphate with respect to total sulphate were found in March and June 2000 (85% and 43%, respectively). The 85% of ammonium-sulphate occurs in the PM fraction <1.5µm, as average (Figure 6-13). Calcium-sulphate shows a bi-modal size distribution with modes in the ranges 1.5-6µm and >24µm, which accounts for 48 and 28 % of calcium-sulphate, respectively (Figure 6-13). This different size distribution of ammonium-sulphate and calcium-sulphate is caused by the diverse formation mechanisms. Ammonium-sulphate is mainly formed by oxidation of gaseous SO_2 and further nucleation to form NH_4HSO_4 and $(NH_4)_2SO_4$ particulates. In contrast, anthropogenic calcium-sulphate may be formed by the reaction of H_2SO_4 with the coarse $CaCO_3$ particulate (Mamane and Gottlieb, 1992; Wu and Okada, 1994). Moreover, calcium-sulphate may be a natural component of soil (gypsum) and may consequently be also emitted by soil re-suspension as a coarse particle.

The size distribution of nitrate experience significant variations throughout the year. In spring (samples of April and May 1999), around 31% of total nitrate occurs in the ranges <1.5µm, 59% in the range <3µm, and 41% in the range >3µm. In summer (samples of June 1999 and 2000) nitrate is mainly found in coarse fractions of PM (>3µm), being around 15% of total nitrate present in the range <1.5µm, 31% in the range <3µm, and 69% in the range >3µm. In winter (samples of January, February and March 2000), in addition to the coarse nitrate, there is an important load of nitrate in the finest ranges of PM (<1.5µm). For these samples, around 59% of total nitrate occur in the range <1.5µm, 73% in the range <3µm, and 27% in the range >3µm. These variations in the size distribution of nitrate are the result of the thermodynamic proprieties of the nitrogenous species and the different possibilities of neutralisation of nitric acid. Thus, the high load of fine (<3µm) nitrate in winter is induced by the enhanced thermal stability of ammonium-nitrate in the cold season (discussed in chapter 5). Moreover, nitrate may also be present as sodium or calcium nitrate, mainly in the warm season (see also chapter 5). The ion balance indicates that total nitrate is distributed among the $(NH_4)NO_3$, $NaNO_3$ and $Ca(NO_3)_2$ species as follow: 4, 25 and 71% in spring (samples of April and May 1999), <1, 29 and 71% in early summer (June 1999 and June 2000) and 42, 3 and 56% in the winter samples (January, February and March 2000). The 92 and 100% of ammonium-nitrate (as average) is present in the ranges <0.7 and <1.5µm, respectively (Figure 6-13). Sodium-nitrate shows a size distribution characterised by a maximum in the range 0.7-6µm which accounts for 56% of total sodium-nitrate (as average, Figure 6-13). Calcium-nitrate showed a maximum in the range 1.5-6µm (47% of calcium-nitrate) with a secondary maximum in the range >24µm (12% of calcium-nitrate, Figure 6-13). This different size distribution of ammonium-nitrate and calcium-nitrate and sodium-nitrate is caused by the diverse formation mechanisms. Ammonium-nitrate is mainly formed by processes of oxidation of gaseous NOx and further nucleation to form particulate NH_4NO_3. In contrast, calcium-

SPRING

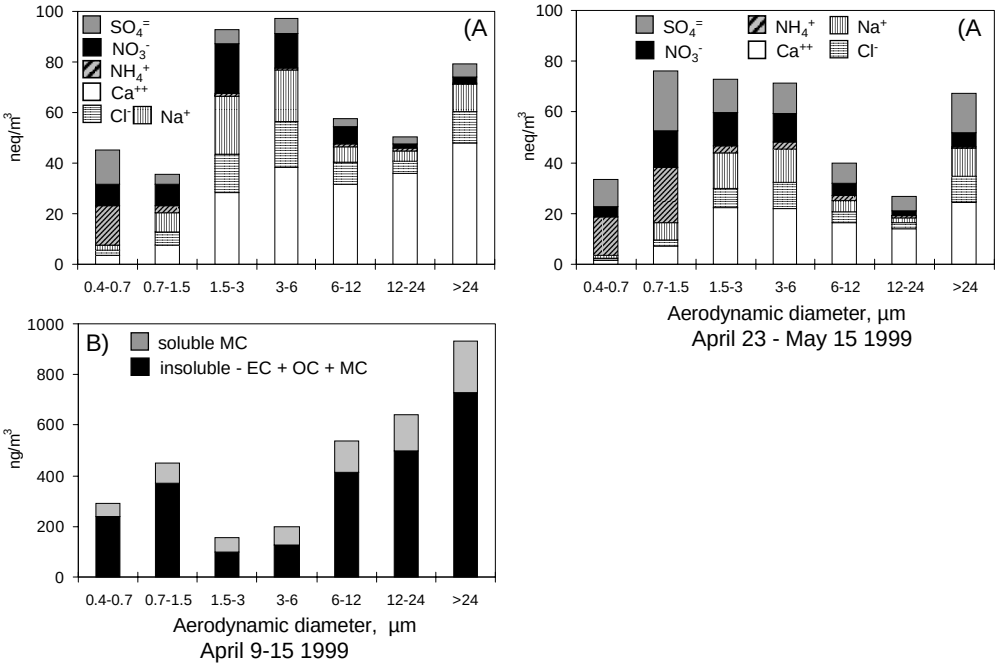

Figure 6-6 Figure 6-7

Figures 6-6 and 6-7. Cascade impactor samples collected in spring 1999. A) water soluble fraction (neq/m^3). B) water soluble and insoluble fractions of carbon. EC, OC and MC: elemental, organic and mineral carbon, respectively.

EARLY SUMMER

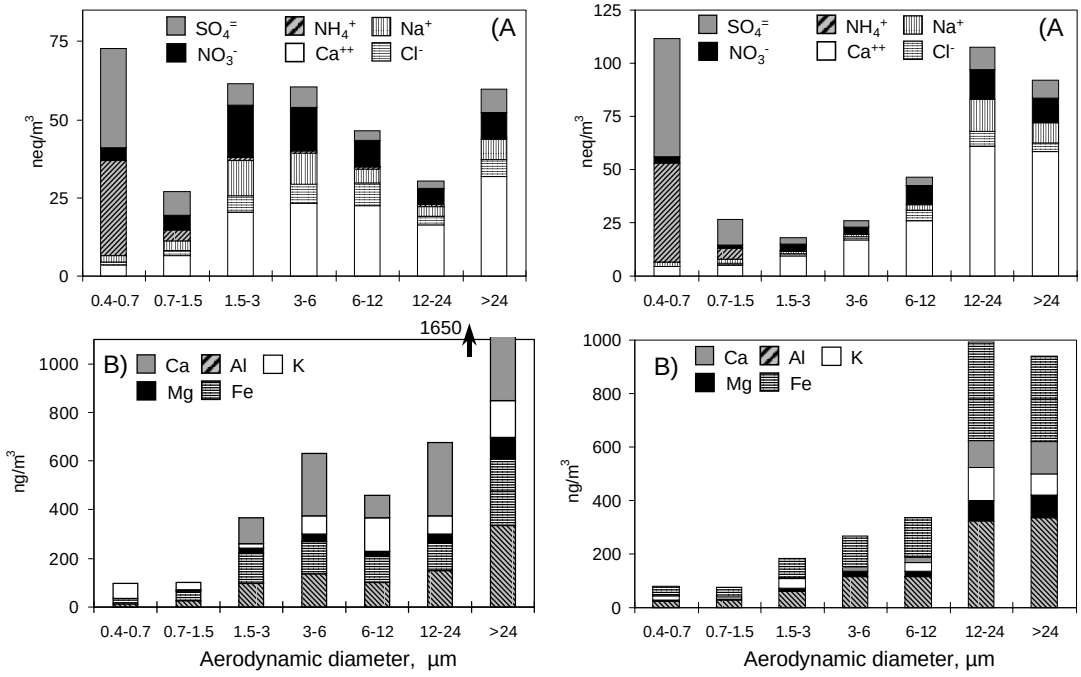

Figure 6-8 Figure 6-9

Figures 6-8 and 6-9. Cascade impactor samples collected in early summer 1999 and 2000. A) water soluble fraction (neq/m^3). B) insoluble fraction (ng/m^3).

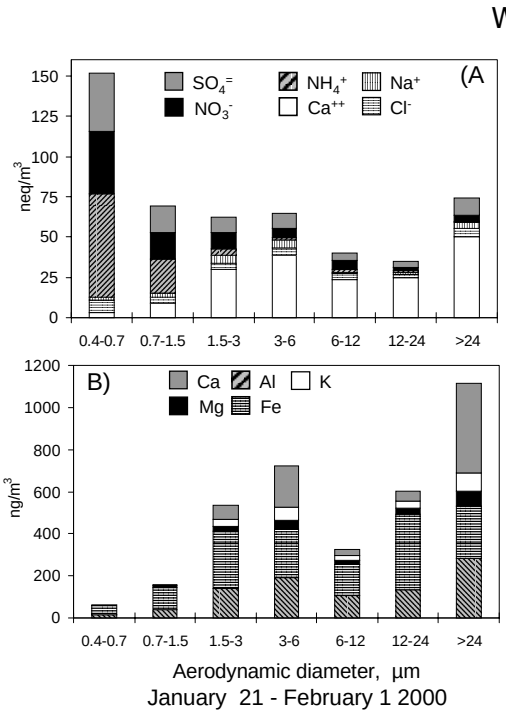

Figure 6-10

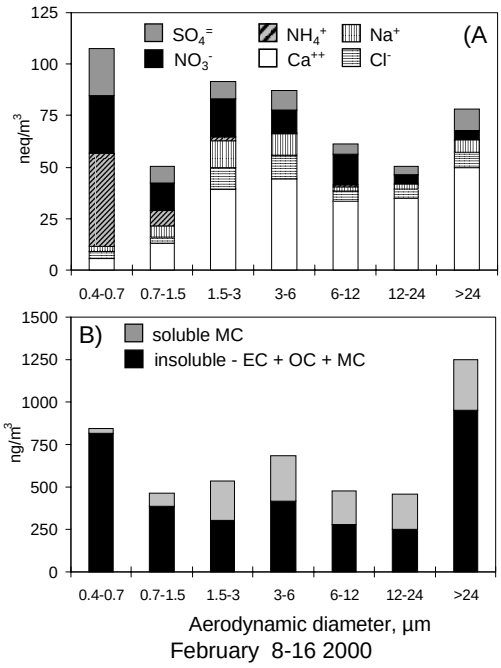

Figure 6-11

Figures 6-10 and 6-11. Cascade impactor samples collected in winter 2000. A) water soluble fraction (neq/m^3). 6-9 B) insoluble fraction (ng/m^3). 6-10 B) water soluble and insoluble fractions of carbon. EC, OC and MC: elemental, organic and mineral carbon, respectively.

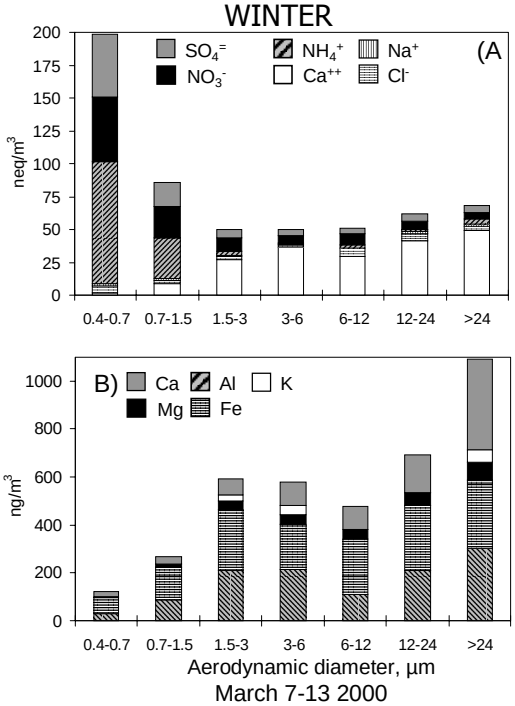

Figures 6-12. Cascade impactor sample collected in March 2000. A) water soluble fraction (neq/m^3). 6-9 B) water insoluble fraction (ng/m^3).

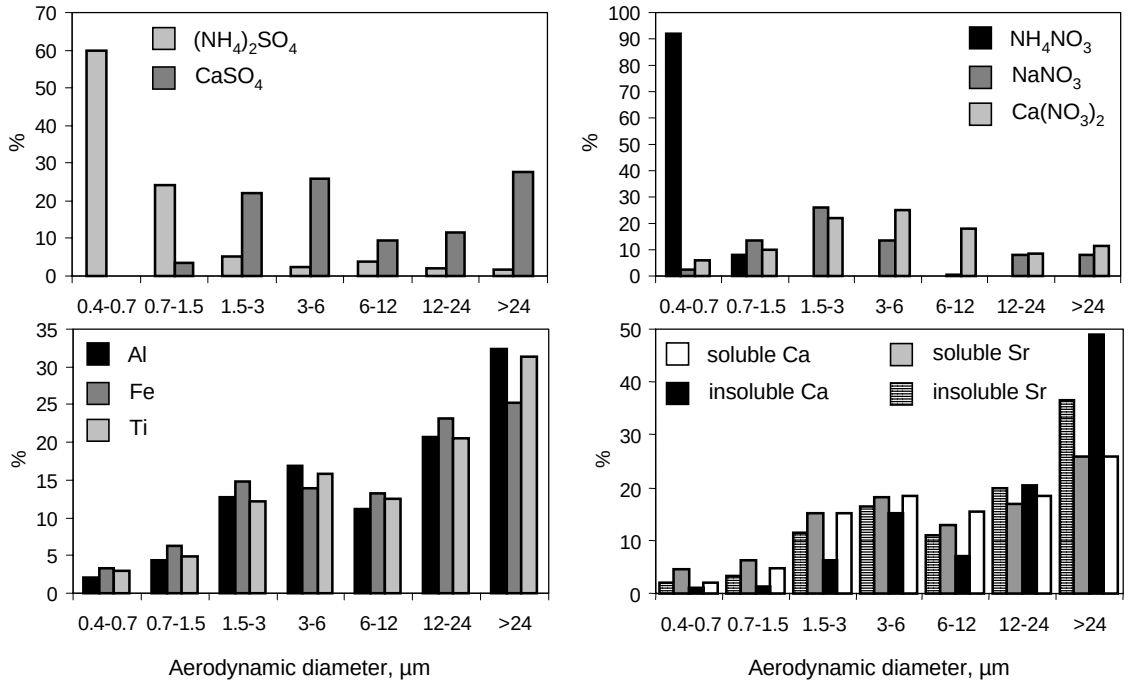

Figure 6-13. Average size distribution of PM species determined by cascade impactor samples.

nitrate and sodium-nitrate are formed by the reaction of nitric acid with coarse calcium-carbonate and sodium-chloride particles, respectively.

Most of Na and Cl, which have a major marine origin, occur in the range >1.5µm. In most samples around 50% of Na and Cl occur in the range 1.5-6µm. However, in winter a significant proportion of Cl (20-25% of total Cl) occurs in the 0.4-0.7µm range, suggesting an anthropogenic origin (also identified in the PM10 and PM2.5 chemical characterisation in chapter 5). In 2 samples a fraction (34 and 63% of total Na and Cl) of Na and Cl was observed in the ranges >12µm. One important finding is the excess of Na with respect to Cl in summer and spring compared with Na/Cl marine ratio. This Na excess accounts for 25-50% of total Na and is mainly observed in the ranges between 0.7 and 6µm. The Na excess is caused by the reaction of acids, such as H_2SO_4 and/or HNO_3, with NaCl, which leads to the formation of gaseous HCl and particulate Na-sulphate and Na-nitrate. Around 80-100% of the Na excess was observed in the range between 0.7 and 6µm, where $NaNO_3$ was previously identified by ion balancing (above discussed).

Most of crustal PM species, such as Ca, Al, Fe, Sr, Ti, Mg, shows a bi-modal size distribution with modes in the ranges 1.5-6µm and >24µm (Figure 6-13). The soluble fraction of Ca and Sr increases from the fine (<0.7µm) to the coarse (>24µm) ranges, whereas the insoluble fraction of these species was not significant in the finest ranges (<1.5µm) of PM (Figure 6-13).

Spring and winter cascade impactor samples were analysed to determine the content in carbon. As stated in chapter 3, the Ca/C ratio in carbonates is used to estimate the load of mineral carbon. Since only the soluble fraction of Ca (which accounts for 80% of the total Ca) was analysed in these spring and winter samples, the content in carbon was classified as "soluble mineral carbon" (sMC) and "insoluble elemental carbon + organic carbon + mineral carbon" (in-

EC+OC+MC). Taking into account the grain-size distribution of the soluble/total Ca concentration ratio determined in other cascade impactor samples, it is estimated that almost the whole in-EC+OC+MC fraction is constituted by EC+OC in the range <1.5μm, and that the EC+OC accounts for 10-50% of in-EC+OC+MC. The in-EC+OC+MC shows a bi-modal size distribution with maximum in the fractions <0.7μm and >24μm. In the winter sample (February 2000 in Figure 6-10) a high load of in-EC+OC+MC is observed in the fraction <0.7 μm, whereas in the spring sample (April 1999 in Figure 6-6) the maximum load of carbon is observed in the fraction >24μm. This seasonal trend is in agreement with the winter EC+OC maximum found in PM10 and PM2.5 (discussed in chapter 5).

6.1.5 Grain-size distribution of PM

A year of continuous measurements with the GRIMM laser spectrometer allowed us to characterise the variations in the grain size distribution of PM on a daily and seasonal basis. The variations in the grain size distribution throughout the day were studied by analysing the size distribution at three different times: night (2:00-4:00 LST average), morning rush hour (8:00-10:00 LST) and afternoon (14:00-16:00 LST). The mean grain size distribution for these periods was calculated for every month between June 1999 and June 2000 (Figure 6-14). Every month, levels of PM with size <20μm were higher during the early morning rush hour (8:00-10:00) than at the night. However, this increase is much more important in levels of coarse particles (>2μm) than in fine particles (<2μm). The mean morning/night PM concentration ratio is 2.8 for PM levels in the range >15μm, 2.5 in the 5-15μm range, 1.6 in the 2-5μm range and 1.2 in the range <2μm. During most of the year, levels of PM in the 5-20μm range decrease from the morning rush hour to the afternoon, and reach the minimum values at night. This daily trend is caused by the previously discussed traffic pattern, which leads to the re-suspension of coarse particles (road dust), and by the longer residence time of the fine particles (<2μm) with respect to the coarser ones.

The analysis of the monthly mean PM grain size distribution also reveals a higher load of PM in the range <0.5μm from January to March 2000 than in the other months. This is correlated with the high loads of ammonium-nitrate and EC+OC observed in the cold season in the TSP segregated fractions in the cascade impactor (discussed above) and in PM10 and PM2.5 (chapter 5).

The aforementioned daily trend of the levels of PM in the different size ranges leads to the previously discussed daily evolution of TSP, PM10, PM2.5 and PM1 levels. Thus, PM2.5/PM10 ratios exhibit minimum values (0.60 to 0.65) in the traffic hours (8:00 to 10:00 h and 18:00 to 21:00 h LST, see Figures 6-15) as a consequence of the re-suspension of coarse road dust (Figure 6-16). Outside these periods, the PM2.5/PM10 ratio is within the 0.75 to 0.85 range because of the sedimentation of the re-suspended coarse fraction. Owing to this re-suspension of coarse road dust and to the longer residence time of fine particles, the amplitude of the daily cycles (maximum minus minimum PM concentration) of TSP and PM10 is much higher than that of PM2.5 and PM1. The mean amplitude from June 1999 to May 2000 was 49μg/m^3 for TSP, 37μg/m^3 for PM10,

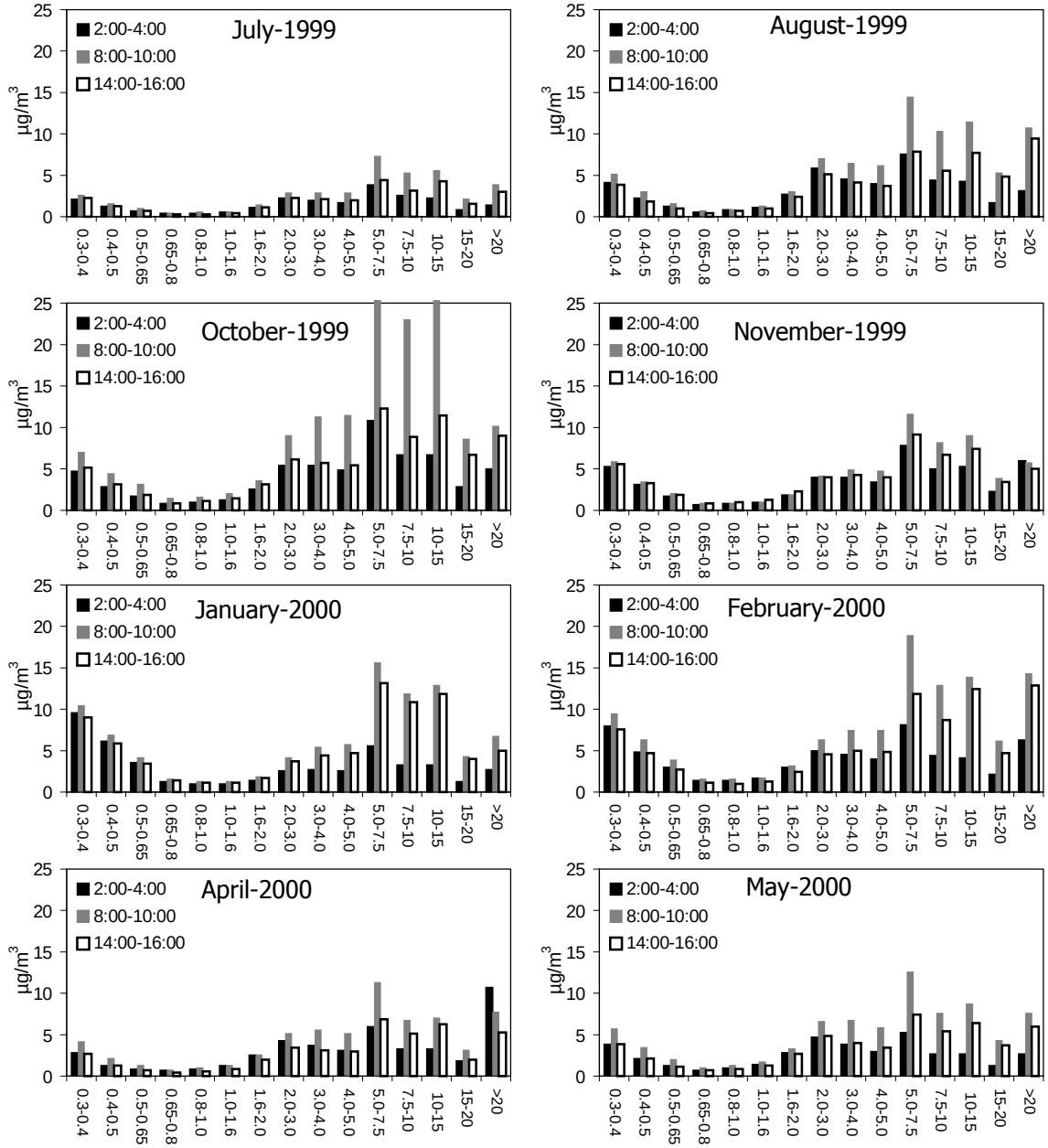

Figure 6-14. Monthly mean grain size in selected periods of the day (hours in LST).

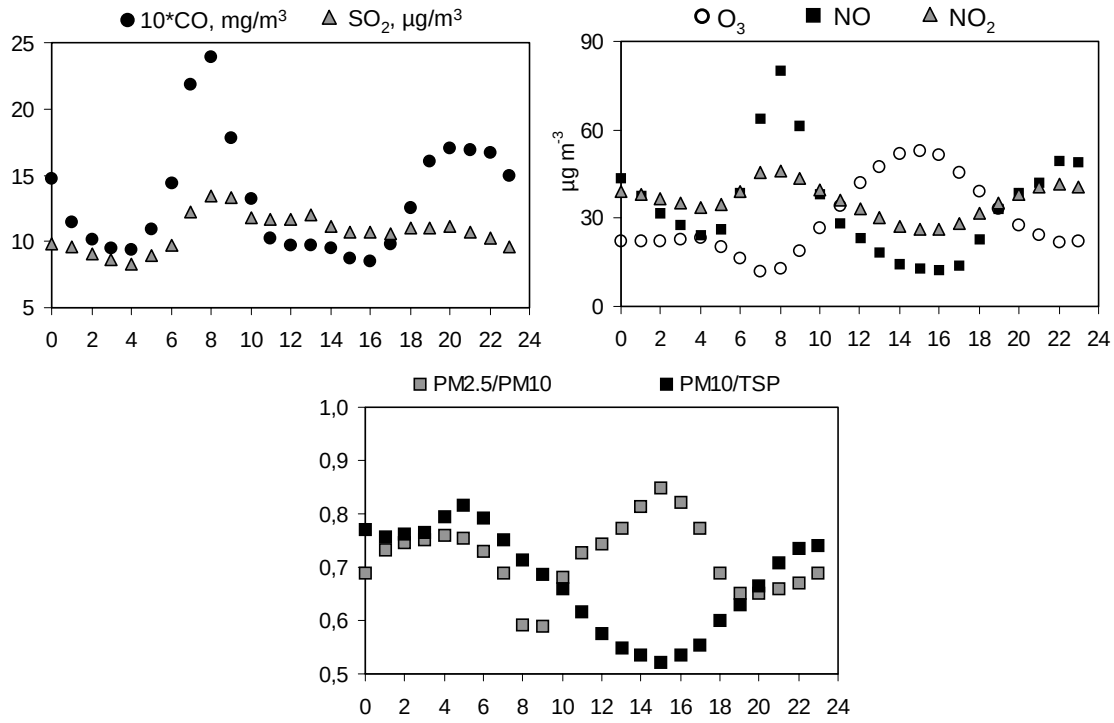

Figure 6-15. Mean hourly levels of major gaseous pollutants and PM10/TSP and PM2.5/PM10 ratios measured recorded at L'HOSPITALET from June 1999 to May 2000.

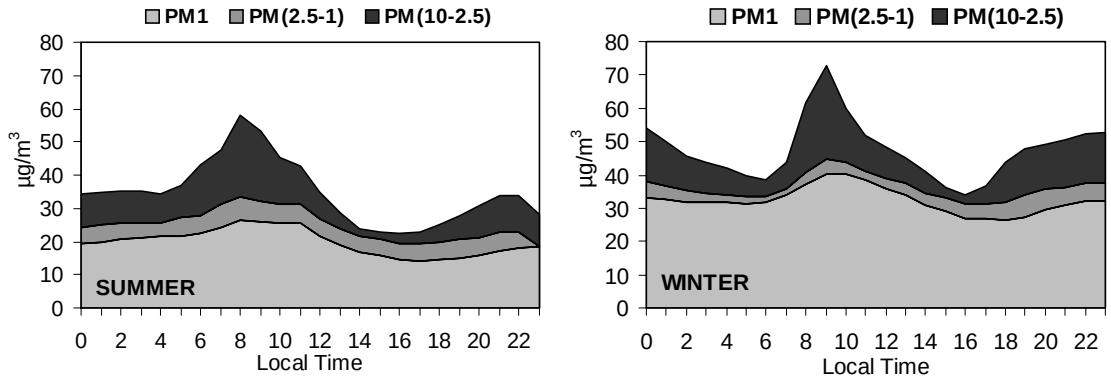

Figure 6-16. Hourly averaged concentrations of PM10, PM2.5 and PM1 in summer (January, February and March averaged) and in winter (July, August and September averaged) periods, highlighting the PM concentrations in the <1µm, 2.5-1 µm and 10-2.5µm ranges.

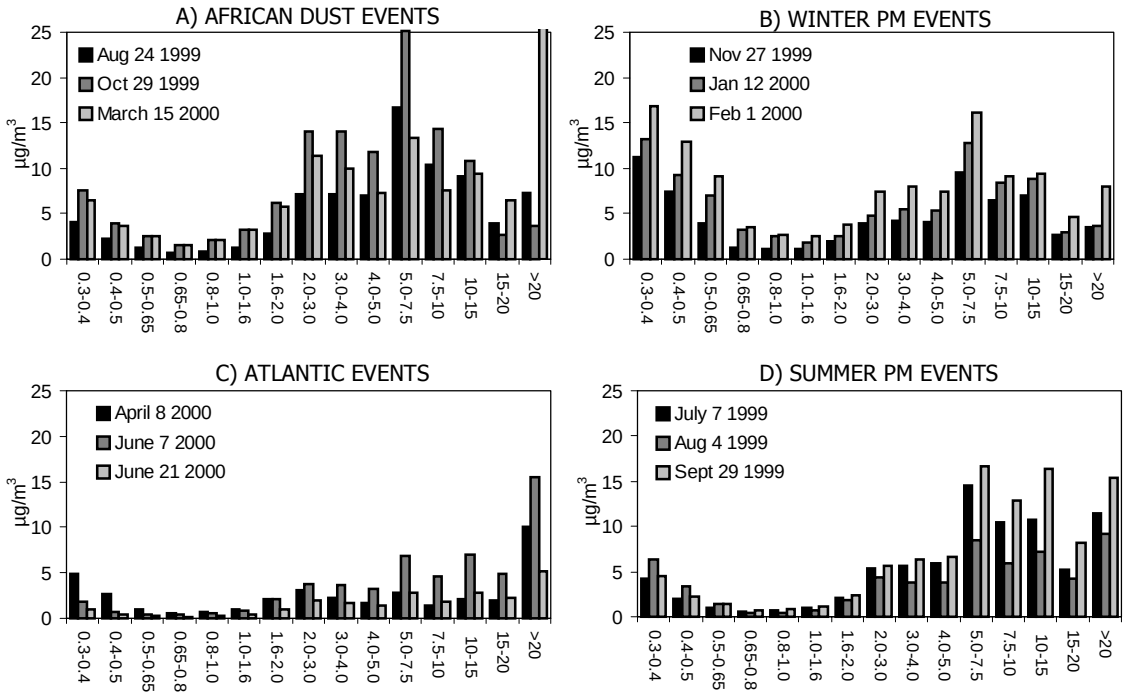

Figure 6-17. Daily mean grain size during selected African dust, winter and summer PM, and Atlantic episodes.

15μg/m^3 for PM2.5 and 13μg/m^3 for PM1. On the other hand, PM10/TSP ratio tends to decrease in the diurnal period (8:00 to 20:00 h LST) when values ranging from 0.50 to 0.65 are measured as a mean for the whole year (Figure 6-15), whereas in the nocturnal period this ratio is close to 0.8. Consequently, it may be assumed that the PM2.5/PM10 ratio is directly dependent on traffic emissions, whereas additional contribution sources for the >10 μm fraction are present in the diurnal period, especially from 10:00 to18:00 h LST. This coarse PM input may be attributed to the inland breeze transport given that the minimal PM10/TSP is recorded at 12:00 GMT (Figure 6-15).

Superimposed on these mean annual trends, sporadic natural PM inputs such as African dust events may significantly reduce the PM2.5/PM10 and PM10/TSP ratios down to 0.5 as a mean daily value, as recorded on several days in August, October and March (Figure 6-17). In contrast, high PM2.5/PM10 (~0.85 as daily mean) and PM10/TSP (~0.90 as daily mean) ratios are recorded during intensive winter PM pollution episodes (Figure 6-17).

6.2 PM characterisation around a large source of secondary particles

6.2.1 The study area

The Teruel coal-fired power station is a relatively high SO_2 emission source located in the Southeast of the Ebro basin in the vicinity of the Iberian (NW-SE) and Catalan (NE-SW) ranges (Figure 6-18). The Teruel power plant is the second highest coal-fired power station in Spain (after As Pontes) and had a mean consumption of 12.000 tonnes of coal per day between 1995 and 1998. The power plant uses electrostatic precipitators which have a 99.95% efficiency for the abatement of primary PM (fly ash). A desulphurisation system has also been in operation since 2000. Owing to use of electrostatic precipitators, the plume is mainly constituted by gaseous pollutants, mainly CO_2 and SO_2. Early studies in this area (Querol et al., 1998a, 1998b, 1999) showed that the freshly emitted SO_2 plume had little impact on PM10 levels. Thus, the SO_2 plume is a source of particulate-sulphate precursors in this region. These SO_2 emissions are dispersed and transformed into sulphate on a regional scale. The conversion rates of these SO_2 emissions to sulphate may undergo daily and seasonal evolutions, with a maximum during daylight and in summer, respectively (Warneck, 1988, and Meszaros, 1999, and references there in). Midday SO_2 oxidation rates ranging from <1%/h in winter to 6%/h in summer have been recorded in this area (Querol et al., 1999b).

The SO_2 emissions occurs in a 348 meters tall stack. The dispersion of the SO_2 plume is highly influenced by the peculiarities of the Mediterranean atmospheric environment. Based on earlier studies (Millán et al., 1992, 1993; Querol et al., 1998a, 1998b, 1999b) the main dispersion patterns are summarised below.

Under advective conditions in winter, NW winds in the Ebro basin predominate, and a narrow plume moves southeastward without spreading being only deformed by mechanical turbulence. In contrast, the plume dispersion in summer is highly influenced by convective processes (thermally activated) and its behaviour is governed by the development of coastal and orographic circulations which undergo a daily evolution. When the Iberian thermal low is developed at noon and in the afternoon in summer, the plume is usually dragged toward the NW. Once the thermal low is relaxed during the evening and night, the transport direction turns towards the eastern and south-eastern sectors. On the following morning the plume changes its dispersion pattern again, as described above. This change usually induces plume impacts on the surface from the previously emitted SO_2 layers. Under very strong convective conditions, with low wind speed, the plume impacts on the surface and induces intensive fumigation episodes in areas close to the power station (<10 km). During intensive episodes the plume may impact on a number of sites around the emission source in a random distribution and the fumigations may occur at short and long distances from the power plant. Thus, in summer the plume has a very erratic bearing and the dispersion pattern shows an intensive daily oscillation. This behaviour accounts for the maximum frequency of SO_2 peak levels on the surface (fumigations) in summer (discussed in chapter 5).

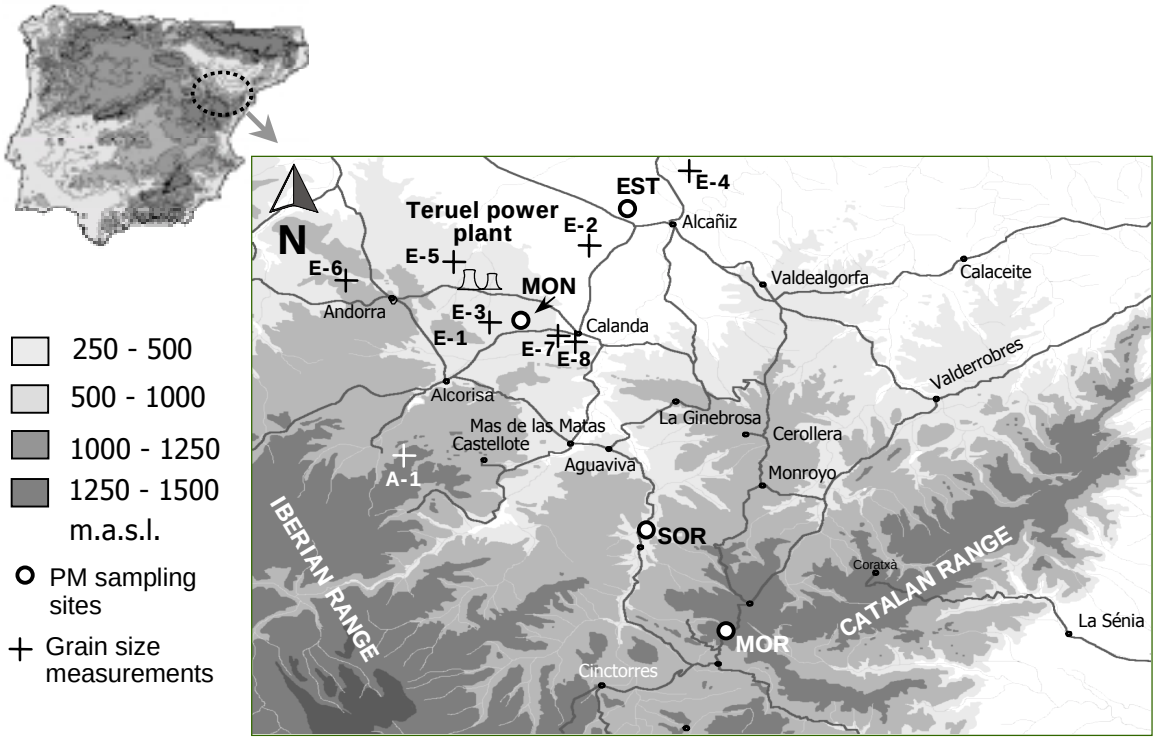

Figure 6-18. Location of the Teruel power plant, the PM10 and PM2.5 sampling stations (MON, EST, SOR and MOR) and the sites where measurements of PM grain size distribution using the GRIMM laser spectrometer mobile unit were performed.

Measurements of emission in the stack of this power plant in 1995 recorded mean concentrations of 11000mg/m^3 and 60mg/m^3 of SO_2 and primary particulate matter, respectively (Querol et al., 1998c). If we consider an oxidation rate of SO_2 to sulphate of 6%/h and a mean wind speed of 10m/s with a constant direction and we ignore the effects of the dilution and deposition, the concentration of sulphate formed in the plume would be 1650mg/m^3 at a distance of 60km from the power station. At this distance from the power station, the ratio "sulphate/primary PM" should be equal to 27.5. Therefore, the Teruel power station is regarded as a large source of secondary particle precursors in this area.

The study area include other PM sources. The Ebro basin is characterised by a semi-arid terrain which favours the re-suspension of soil dust in summer. Pig-farming is the main livestock activity in the region and is a significant source of ammonia. Moreover, crop cultivation and sheep and goat grazing could also eventuality contribute to the soil re-suspension in the Ebro basin. The Iberian and Catalan ranges include both large forests and semi-arid areas, and cultivation of crops and grazing. Furthermore, the study area is also affected by PM transported from distant urban/industrial sites (e.g. the coastal area or inland cities such as Zaragoza or Teruel) during Regional episodes and by North African dust.

6.2.2 Sampling and measurements

The following sampling and measurement sites (Figure 1-18 and Table 6-1) were selected on the basis of their location with respect to the Teruel power station, to the main directions of the SO_2 plume transport and the micro-climatic areas:

The MONAGREGA station is located at a semi-arid rural site in the Ebro basin. This station is situated 7.6Km to the SE of the power station and is influenced by the fresh SO_2 emissions mainly in the late morning and noon. The breeze blows from the NNE during daylight (up-slope wind on the southern slope of the Ebro basin) and from the NW at night (channelled airflow along the Ebro basin).

The ESTANCA station is located at a semi-urban rural site in the Ebro basin. The site is situated 18.5Km to the NE of the power station and is affected by fresh SO_2 emissions mainly in the late morning and noon. The breeze blows in a direction similar to that at MONAGREGA.

The SORITA station is located in the bottom of a valley in the Iberian range. This is also a rural site placed 34km to the SE of the power station.

The MORELLA station is located at the top of a mountain of the convergence of the Iberian and Catalan ranges. The site is placed 46.8Km to the SE of the power station. The breeze blows from the SE during daylight (up-slope wind on the coastal slope of the Catalan range) and from NW during night (channelled airflow from the Ebro basin).

Meteorological data from the air quality monitoring stations of VILAFRANCA, MORELLA and SORITA and from the Teruel power station were used to differentiate the periods characterised by breeze or advection of air masses.

At these four fixed stations, 8-hours sample of PM were taken twice per day, as representative of the nocturnal (from 23:00 to 7:00 LST) and diurnal (from 11:00 to 19:00 LST) periods. From July 16 to 21 2000, the emphasis was on the chemical characterisation of PM10. To this end diurnal and nocturnal samples of PM10 were simultaneously collected at the four fixed stations. From July 24 to 27 2000 the focus was on the PM10 and PM2.5 sampling. Thus, diurnal and nocturnal PM10 and PM2.5 samples were collected at the MONAGREGA station. At MORELLA, the two PM10 samples per day were uninterruptedly taken from July 16 to 27 2000. Moreover, a sample of TSP size segregated fractions was collected at MONAGREGA from July 16 to 21 2000.

In addition to the above PM10 and PM2.5 sampling strategy in ambient air, PM10 and PM2.5 samples were also collected during fumigations of the SO_2 plume when this plume impacted on the surface. The monitoring of the direction of transport of the SO_2 plume and the fumigation on the surface were performed with a COSPEC (correlation spectrometer system) SO_2 analyser mobile unit (which provides data on the SO_2 vertical load) and a conventional SO_2 monitor (which provides data on the SO_2 concentrations at the surface levels based on the pulsed fluorescence SO_2 analysis) following the methodology described by Millán et al. (1993, 1998).

The sampling of PM10 and PM2.5 was carried out by means of high volume samplers (DH-80 at the rate of $30m^3/h$, MCV-CAF at the rate of $30m^3/h$ or GRASEBY-ANDERSEN at the rate of

Table 6-1. Location of the stations for PM sampling and monitoring.

Sampling site	Location	Altitude	Latitude	Longitude
MONAGREGA	Ebro basin (rural)	537 m	40º56'42"N	00º17'26"W
ESTANCA	Ebro basin (rural)	522 m	41º03'30"N	00º11'20"'W
SORITA	Iberian range (rural, bottom of valley)	640 m	40º44'06"N	00º10'10"W
MORELLA	Catalan range (rural, top of mountain)	1156 m	40º38'35"N	00º05'37"E

Table 6-2. Location of mobile station for grain-size analysis of TSP with the GRIMM laser spectrometer around different PM emission sources (E) and ambient air measurements (A).

Nº	Measurement description	Latitude	Longitude
	PM sources		
E-1a	Fumigation of the SO_2 plume from Teruel power station	40º57'54"N	00º25'15"W
E-1b	Fumigation of the SO_2 plume from Teruel power station	40º55'51"N	00º19'41"W
E-1c	Fumigation of the SO_2 plume from Teruel power station	40º57'54"N	00º25'15"W
E-2	Natural re-suspension on arid soil	41º02'10"N	00º11'01"W
E-3	Soil re-suspension caused by crop cultivation	40º56'51"N	00º17'33"W
E-4	Soil re-suspension caused by grazing (sheep)	41º02'50"N	00º09'15"W
E-5	Re-suspension on coal piles caused by wind	40º59'54"N	00º22'46"W
E-6	Fugitive emissions from the Barrabassa mine	40º59'31"N	00º28'51"W
E-7	Emissions from a chamotte factory	40º56'18"N	00º14'32"W
E-8	Emissions from a gypsum factory	40º56'27"N	00º14'26"W
	Ambient air		
A-1	Iberian range mountain background at noon July 18	40º48'43"	00º25'36"W
A-2	Ebro basin (non fumigation at E-1a and c site) July 20	40º57'54"N	00º25'15"W
A-3a	Ebro basin (MONAGREGA) night-time July 19 2000	40º56'42"N	00º17'26"W
A-3b	Ebro basin (MONAGREGA) night-time July 20 2000	40º56'42"N	00º17'26"W
A-3c	Ebro basin (MONAGREGA) July 21-24 2000	40º56'42"N	00º17'26"W
A-3d	Ebro basin (MONAGREGA) July 24-25 2000	40º56'42"N	00º17'26"W
A-3e	Ebro basin (MONAGREGA) July 25-27 2000	40º56'42"N	00º17'26"W
A-4	Ebro basin (SORITA) night-time 21 July 2000	40º44'06"N	00º10'10"W

69m^3/h) equipped with PM10 and PM2.5 cut-off inlets (DIGITEL, MCV or GRASEBY-ANDERSEN depending on the station) and quartz glass filters (QF20 Schleicher and Schuell). The sampling of TSP grain-size fractions (7 stages from 0.3 to >20µm) was performed by means of a Retsch PI-1 cascade impactor. Once the levels of bulk particulates were obtained by weighting the filters using standard procedures, filters and cascade impactor samples were chemically analysed to determine levels major and trace species following the procedures described in chapter 3.

At the four fixed monitoring stations (Table 6-1) levels of PM were continuously monitored by means of PM10 measurements carried out with TEOM (Rupprecht and Patashnick) equipment at the MONAGREGA and the ESTANCA stations, TSP measurements performed by means of a beta-attenuation equipment (Dasiby) at MORELLA, and PM10, PM2.5 and PM1 measurements performed with a laser spectrometer dust monitor GRIMM 1107 (Labortechnik GmbH & Co. KG) at SORITA. Furthermore, additional automatic measurements of atmospheric particulate levels and grain-size

Table 6-3. Classification of the periods during the sampling campaign in accordance with the main meteorological scenarios. H(A+WE): anticyclone over the Atlantic and Western Europe; WGC(WM): weak gradient conditions over the Western Mediterranean; ITL: Iberian thermal low.

Dates	Pressure pattern	Local winds	Air mass origin	Type of event
July 15-18	H(A+WE)	NW-advection	NW-Atlantic	Atlantic
July 18-22	WGC(WM)+ITL+H(A+WE)	Breeze / SE	Regional	Regional
July 23	L(P)	S- advection	North Africa	African
July 24-26	L(A)	W-advection	W-Atlantic	Atlantic
July 27-28	WGC(WM)+ITL	Breeze / SE	Regional	Regional

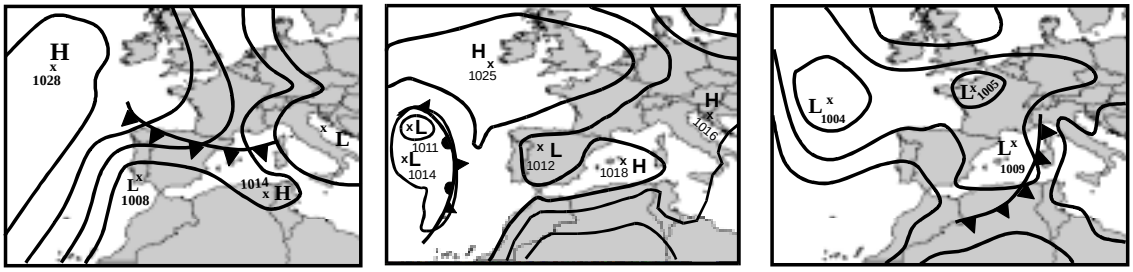

A) 00UTC July 16 2000 B) 18UTC July 19 2000 C) 06UTC July 24 2000

Figure 6-19. Synoptic charts of pressure (mb) at sea level during selected dates of July 2000.

distribution were carried out with the laser spectrometer dust monitor GRIMM 1108 (Labortechnik GmbH & Co. KG) in ambient air at different fixed stations, in the SO_2 plume (simultaneously with the PM10 and PM2.5 sampling) and around specific particulate matter sources emission (Table 6-2). This dust monitor determines the particulate matter levels in 15 different grain-size channels from 0.3 to >20 μm.

6.2.3 Meteorological scenarios

During the measurement campaign meteorological scenarios inducing Regional PM episodes and advections of Atlantic and North African air masses were concatenated (Table 6-3). In the periods July 15-17 and 24-26 advection of NW and W Atlantic air masses took place, respectively. In July 15 and 16, and 24 Atlantic cold fronts reached the study area (Figures 6-19 A and C) inducing depletion in the ambient temperature. From July 18 to 22 weak gradient conditions over the Western Mediterranean favoured the increase in the temperature, the breeze circulation at the coastal and mountain sites (Figure 6-20) and the Iberian thermal low development (Figure 6-19B). This is the scenario for the typical summer transport patterns of the SO_2 plume and the Regional PM episodes (discussed in chapter 4). On July 23 the western end of a large African dusty air mass transported over the Mediterranean reached the study area (Figure 6-21). On July 27 a smooth Regional episode began to be developed.

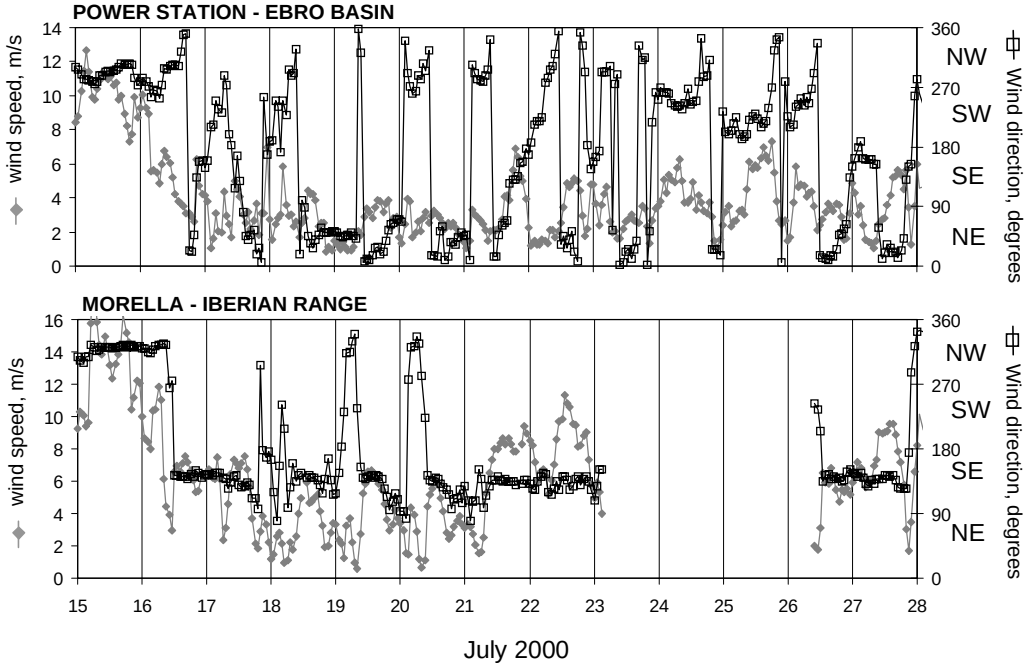

Figure 6-20. Hourly values of wind speed and velocity recorded at MORELLA in the confluence of the Iberian and Catalan ranges and at the Teruel power station in the Ebro basin from July 15 to 23 2000.

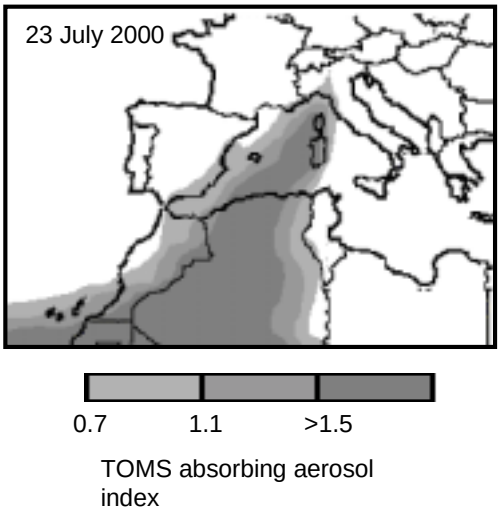

Figure 6-21. TOMS map of absorbing aerosol index for July 23 2000.

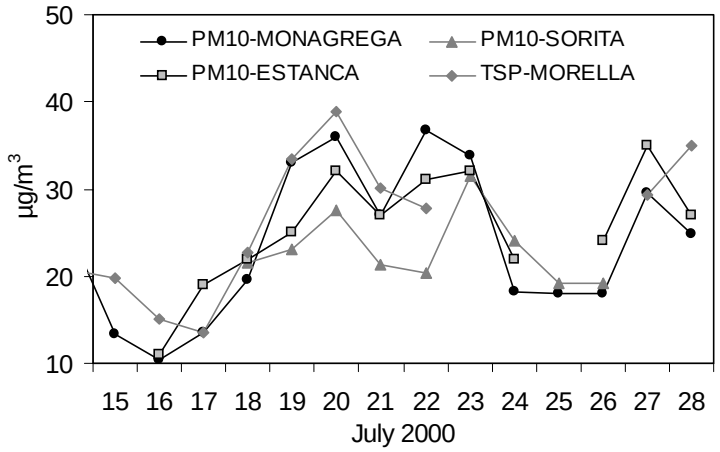

Figure 6-22. Daily mean PM10 and TSP concentrations in the second half of July 2000.

6.2.4 PM10 & PM2.5 ambient levels

Figure 6-22 shows the daily mean values of PM10 and TSP (see O_3 and temperature in Figure 4-20 of chapter 4) recorded during the campaign at the air quality monitoring stations. The lowest and highest PM levels were recorded during the Atlantic and Regional episodes (see dates in Table 6-3), respectively.

Table 6-4 shows the diurnal and nocturnal mean levels of PM10 components in the period July 16-21 2000, when PM10 was simultaneously sampled at four stations. In this period, mean levels of most of the crustal components were higher at the sites placed in the Ebro basin (MONAGREGA and ESTANCA) than in the Iberian and Catalan ranges (SORITA and MORELLA). The mean Ebro-basin/range ratio concentrations was 2.0 for Sr, 1.7 for Ca and $CO_3^=$, 1.4 for Mg, 1.2 for Fe, Al_2O_3 and SiO_2 and 1.1 for Ti. Most of the crustal components exhibited the highest levels at ESTANCA or MONAGREGA and the lowest levels at MORELLA (Ca, Fe, Mg, Al or Sr). Mean levels of nss-$SO_4^=$ were slightly higher at MONAGREGA and SORITA than at ESTANCA, whereas the lowest levels were recorded at MORELLA. Mean levels of NO_3^- were slightly higher in ESTANCA than in the other stations. Levels of OC+EC at the Iberian/Catalan range were no significantly different from those recorded at the Ebro basin.

Some of the major PM10 components presented a daily evolution (Table 6-4). A number of the crustal components (e.g. Ca, $CO_3^=$, Al_2O_3, SiO_2 and Fe) showed higher levels during daylight than at night (Figure 6-23) owing to the re-suspension of crustal PM from semi-arid soils. This daily evolution was enhanced during the Regional PM episode (July 18 to 21; Figure 6-22 and Table 6-3) owing to the fact that the high temperatures favour the turbulence dynamics on the dry soils. Mean levels of nss-sulphate were also higher during daylight (Table 6-4). This daily evolution was also enhanced during the Regional episode (July 18-21 2000; Figure 6-24A), whereas during the periods of air mass advection no significant daily cycles were detected. Nss-$SO_4^=$ mainly occurs as

Table 6-4.A,B). Mean diurnal and nocturnal major and trace elements and bulk PM10 levels (in ng/m^3) obtained in the period July 16-21 at MONAGREGA and ESTANCA. N, number of samples. The source apportionment (in ng/m^3) of PM10 include the crustal source, secondary particulates (ammonium sulphate and nitrate), organic+elemental carbon (OC+EC) and sea spray (Na +Cl+ss-$SO_4^=$).

July 16-21	A) MONAGREGA		July 16-21	B) ESTANCA	
PM10	night	daylight	PM10	night	daylight
	23:00-7:00	11:00-19:00		23:00-7:00	11:00-19:00
PM10	24489	36019	PM10	24251	28784
Ca	489	787	Ca	643	698
Al_2O_3	514	674	Al_2O_3	442	436
SiO_2	1286	1684	SiO_2	1105	1091
Fe	97	118	Fe	105	134
Mg	126	126	Mg	167	161
K	123	113	K	147	135
OC+EC	4756	4752	OC+EC	4231	4301
$CO_3^=$	734	1180	$CO_3^=$	965	1048
Na	640	535	Na	817	644
Cl	427	357	Cl	545	430
ss-$SO_4^=$	160	134	ss-$SO_4^=$	204	161
nss-$SO_4^=$	5437	10358	nss-$SO_4^=$	5366	8866
NO_3^-	2090	1261	NO_3^-	2718	1660
NH_4^+	2215	3582	NH_4^+	2092	3367
Zn	49	47	Zn	53	37
Ti	8	14	Ti	8	8
P	8	17	P	21	12
Pb	10	9	Pb	9	9
Ba	40	41	Ba	48	20
Sr	3	5	Sr	3	3
Mn	2	3	Mn	3	4
Ni	4	4	Ni	<1	2
Cu	4	3	Cu	17	8
V	4	4	V	3	4
Cr	<1	<1	Cr	<1	2
N samples	5	5	N samples	5	5
Σcomponents	18990	25445	Σcomponents	19714	23241
Determined %	77	71	Determined %	81	81
Crustal	3428	4759	Crustal	3654	3746
Secondary	9742	15201	Secondary	10177	13893
OC+EC	4756	4752	OC+EC	1948	2542
Marine	1228	1026	Marine	1566	1235

Table 6-4.C,D). Mean diurnal and nocturnal major and trace elements and bulk PM10 levels (in ng/m^3) obtained in the period July 16-21 at SORITA and MORELLA. N, number of samples. The source apportionment (in ng/m^3) of PM10 includes the crustal source, secondary particulates (ammonium sulphate and nitrate), organic+elemental carbon (OC+EC) and sea spray (Na +Cl+ss-$SO_4^=$).

July 16-21	C) SORITA		July 16-21	D) MORELLA	
PM10	night 23:00-7:00	daylight 11:00-19:00	PM10	night 23:00-7:00	daylight 11:00-19:00
PM10	19639	27814	PM10	22694	29213
Ca	257	573	Ca	370	379
Al_2O_3	434	587	Al_2O_3	329	322
SiO_2	1084	1468	SiO_2	822	804
Fe	68	140	Fe	96	89
Mg	106	121	Mg	79	117
K	142	156	K	143	180
CO+CE	4093	6546	CO+CE	4460	5519
$CO_3^=$	386	860	$CO_3^=$	555	568
Na	597	614	Na	689	789
Cl	398	409	Cl	459	526
ss-$SO_4^=$	149	153	ss-$SO_4^=$	172	197
nss-$SO_4^=$	4900	10900	nss-$SO_4^=$	4332	7454
NO_3^-	1844	1208	NO_3^-	1959	1682
NH_4^+	1967	2952	NH_4^+	1588	2263
Zn	76	69	Zn	105	99
Ti	5	10	Ti	11	10
P	25	9	P	6	13
Pb	14	21	Pb	13	24
Ba	52	21	Ba	ND	ND
Sr	2	2	Sr	2	2
Mn	2	3	Mn	3	2
Ni	<1	<1	Ni	3	2
Cu	5	5	Cu	10	16
V	3	4	V	3	4
Cr	<1	<1	Cr	<1	<1
N samples	5	5	N samples	5	5
Σcomponents	16226	26424	Σcomponents	13869	21068
Determined %	83	103	Determined %	79	81
Crustal	2560	3949	Crustal	2411	2483
Secondary	8711	15060	Secondary	10001	16926
OC+EC	4093	6546	OC+EC	ND	ND
Marine	1145	1176	Marine	1320	1513

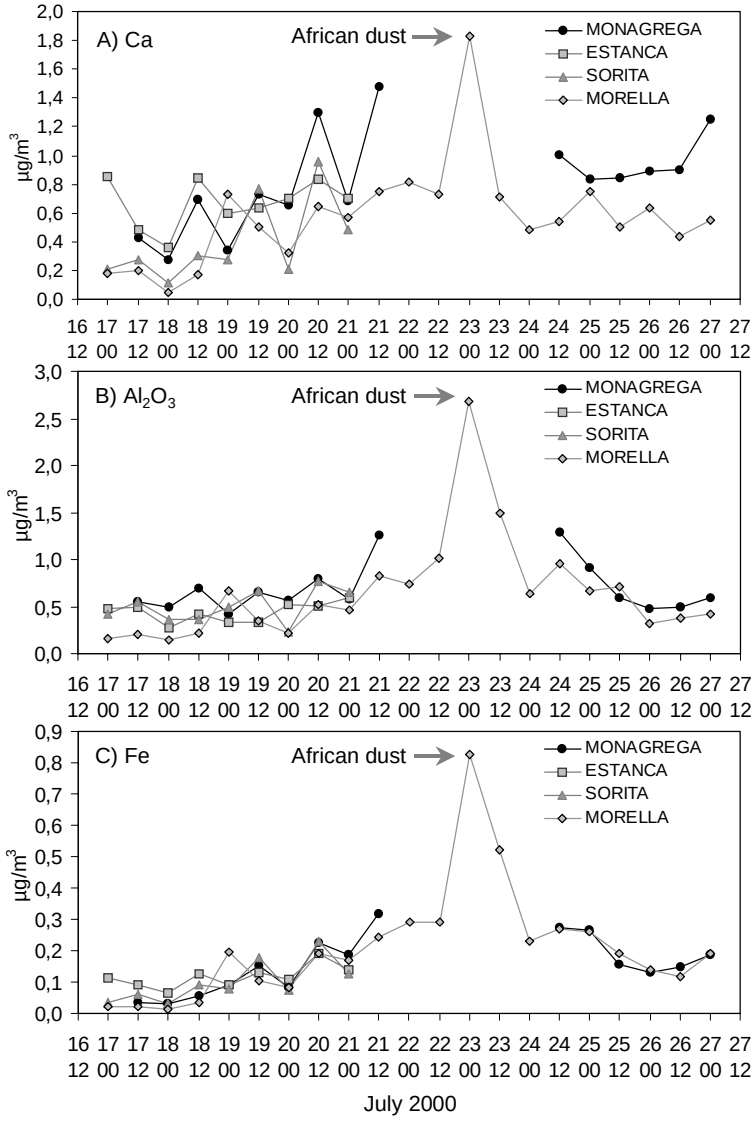

Figure 6-23. Diurnal (labelled with 12) and nocturnal (labelled with 00) mean levels of Ca, Al_2O_3 and Fe in PM10 at the fixed stations from July 17 to 27 2000.

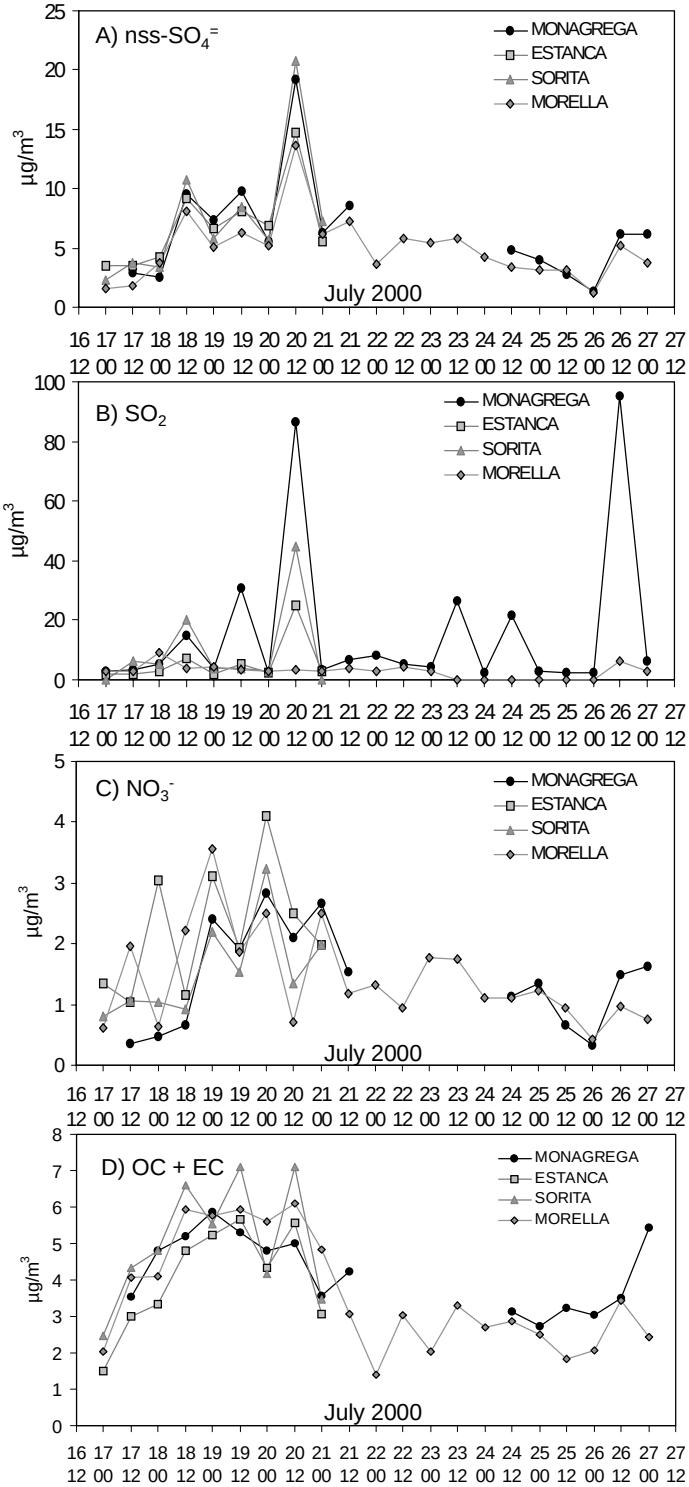

Figure 6-24. Diurnal (labelled with 12) and nocturnal (labelled with 00) mean levels of nss-$SO_4^=$, SO_2 and NO_3^- in PM10 at the fixed stations from July 17 to 27 2000.

ammonium-sulphate (Figure 6-25A). The higher daylight nss-sulphate levels are attributed to the enhanced amount of SO_2 at the ground level due to the SO_2 plume abatements (Figure 6-24B) and to the enhanced nss-sulphate photochemical formation. Conversely, NO_3^- exhibited higher mean levels during night-time than daylight (Figure 6-24C). This daily evolution of nitrate is attributed to the influence of temperature on the gas/particle partitioning of nitric acid, ammonia and ammonium-nitrate (Meszaros, 1999 and references therein, see also chapter 5): $HNO_3(g)+NH_3(g) \leftrightarrow NH_4NO_3(s \text{ or } aq)$. Higher daylight temperatures favour the occurrence of gaseous - nitric acid (HNO_3), whereas nocturnal cooling allows the occurrence of ammonium-nitrate. Thus, during daylight nitrate occurs probably as calcium or sodium nitrate, whereas at night an additional ammonium-nitrate is present. Levels of OC+EC showed a daily cycle characterised by higher levels during daylight than during the night at SORITA and MORELLA.

Figure 6-26 shows the hourly averaged PM10 and TSP levels at the four selected monitoring stations. PM levels were higher during daylight at night. The increase in the PM10 concentrations during daylight is favoured by the increase in the load of crustal PM and to the enhanced formation of ammonium-sulphate during daylight. At SORITA and MORELLA, levels of OC+EC also increased during daylight. The decline in the nocturnal PM levels are favoured by coarse PM deposition. Moreover, the daylight increase in PM levels is typically associated with the inland/up-slope breeze blowing which are conducive to an inland/up-ward transport of pollutants. The nocturnal decrease in PM levels is also favoured by the seaward/down-slope airflow.

At MORELLA and SORITA (in the Iberian and Catalan ranges), PM levels decreased after mid-afternoon (18:00 LST), whereas at MONAGREGA and ESTANCA (in the Ebro basin) a maximum in PM levels was recorded between 19:00 and 21:00 (LST). This significant difference in the daily PM cycle, is probably related to the different air mass dynamics at the top of the ranges and in the Ebro basin in the late afternoon. At the MORELLA station (at the top of the range), the up-slope wind (from the coastal slope) typically blows from 11:00 to 19:00 (LST), whereas in the Ebro basin the NNE up-slope wind typically blows from 11:00 to 21:00, and frequently up to 23:00 (LST). Thus, from 19:00 to 21:00 the up-ward transport of PM ceased in the Iberian and Catalan ranges, whereas the NNE up-slope wind continues to favour the PM transport from the lower levels of the Ebro basin to the MONAGREGA and ESTANCA sites (probably NO_3^- and OC+EC from the small towns located in the basin and from the large urban sites on the coast in the context of the Regional episodes). See July 18 and 19 2000 in Figure 6-27, where PM and SO_2 levels and wind speed and direction are plotted from July 17 to 21. Note that there is no correlation between PM and SO_2 levels and consequently fresh emissions from the Teruel power plant are not involved in the PM daily cycles.

In addition to the aforementioned daily cycles, the PM10 components and the bulk PM10 levels showed an increasing trend from July 17 to 21 (Figures 6-21, 6-22 and 6-23). This is attributed to the accumulation of PM due to the scarce renovation of the air masses associated with the breeze circulation. This scarce air mass renovation also contributes to the enhancement of

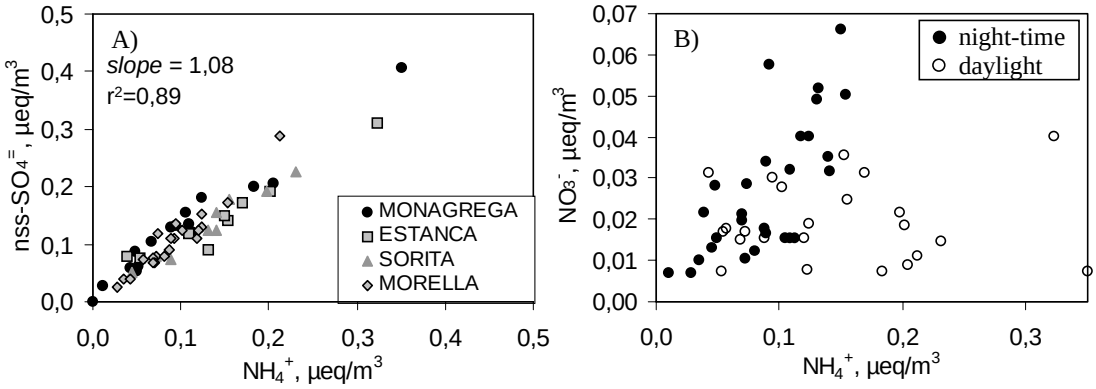

Figure 6-25. Nss-$SO_4^=$ (A) and NO_3^-(B) versus ammonium in PM10 samples taken in ambient air at the fixed stations (Table 1) from July 16 to 27 2000.

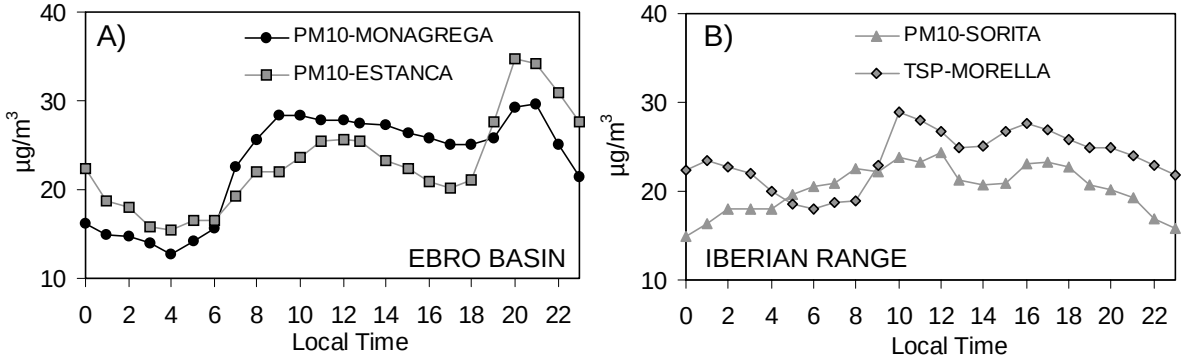

Figure 6-26. Hourly mean levels of PM10 and TSP from July 16 to 21 2000 at the fixed stations.

the daily cycles by the aforementioned mechanisms (accumulation of PM components and its gaseous precursors, re-suspension of crustal PM and enhanced levels of photo-oxidants). After July 21, non of the PM10 components at MONAGREGA and MORELLA showed significant daily cycles (Figures 6-22 and 6-23) owing to the prevalence of mass advections. The most important feature of the time series of the levels of crustal components at MORELLA is the peak concentration on July 23 caused by the aforementioned African dust outbreak (Figure 6-21).

Table 6-5 shows the diurnal and nocturnal mean levels of PM10 and PM2.5 components from July 24 to 27 2000 at MONAGREGA and MORELLA (Figure 6-23 and 6-24). The analysis of these data shows that:

1) the mass of nss-sulphate is mainly (~98% of nss-sulphate) in the fine fraction (<2.5µm) of PM10,

2) the mass of the soil components is mainly (~ 80% of Fe, 79% of Al_2O_3 and SiO_2, 76% of Mg, 76% of Ti and Sr, 70% of Ca and $CO_3^=$) in the coarse fraction (2.5-10µm) of PM10,

3) the mass of the marine components is mainly (~77% of Na and 80% of Cl) in the coarse fraction of PM10,

4) the mass of nitrate is mostly (82% of NO_3^-) in the coarse fraction of PM10 as sodium and calcium nitrate,

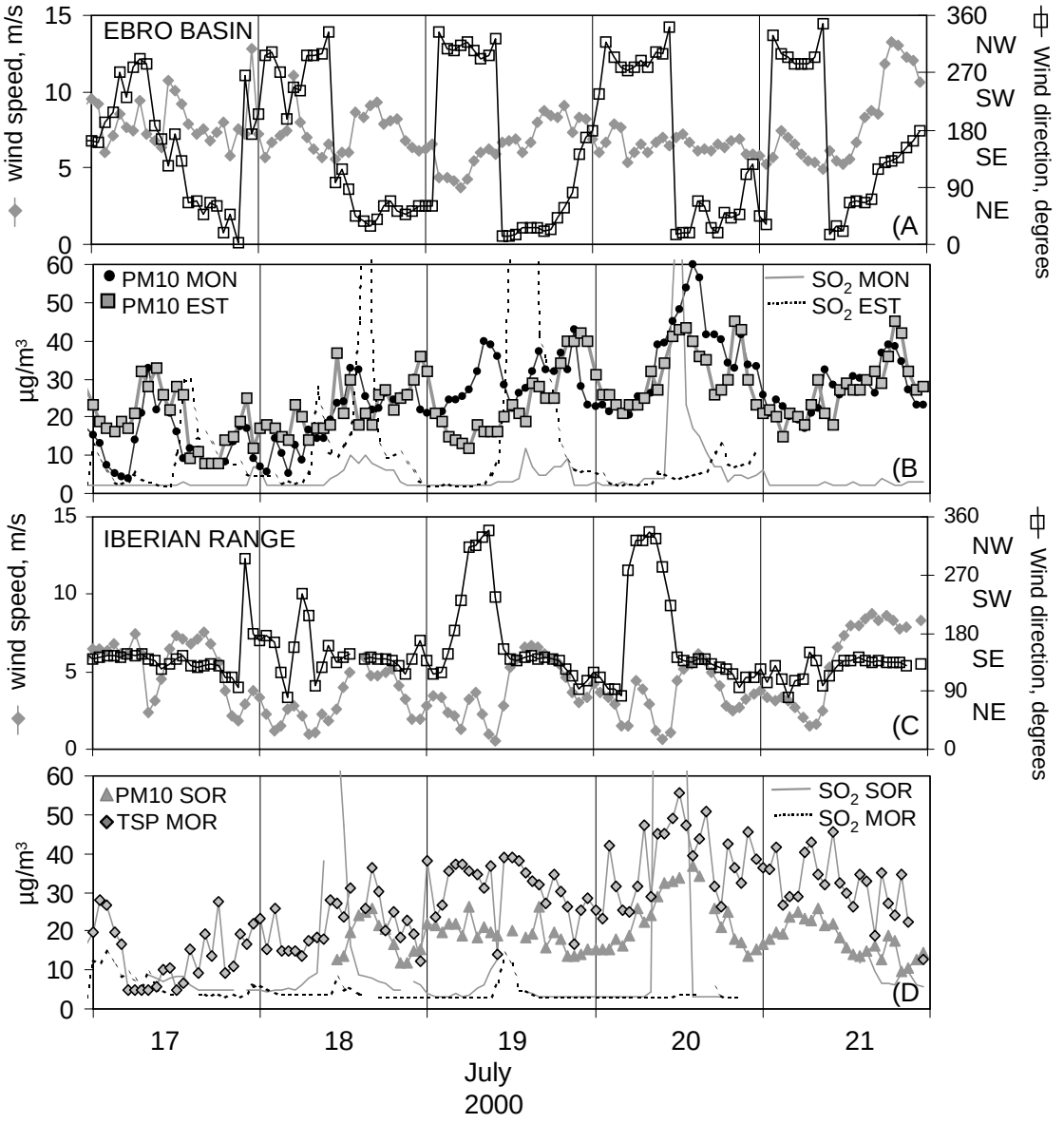

Figure 6-27. Hourly wind speed and direction and TSP, PM10 and SO_2 levels at sites located in the Ebro basin (MONAGREGA and ESTANCA) and the Iberian and Catalan ranges (MORELLA and SORITA).

Table 6-5.A,B). Mean diurnal and nocturnal major and trace elements and bulk PM10 and PM2.5 levels (in ng/m^3) obtained in the period July 24-27 at MONAGREGA. N, number of samples. The source apportionment (in ng/m^3) of PM10 includes the crustal source, secondary particulates (ammonium sulphate and nitrate), organic+elemental carbon (OC+EC) and sea spray (Na +Cl+ss-$SO_4^=$). ND: no data.

July 24-27	A) MONAGREGA		July 24-27	B) MONAGREGA	
PM10	night 23:00-7:00	daylight 11:00-19:00	PM2.5	night 23:00-7:00	daylight 11:00-19:00
PM10	17646	17418	PM2.5	12809	13656
Ca	990	916	Ca	272	304
Al_2O_3	663	791	Al_2O_3	185	116
SiO_2	1658	1977	SiO_2	464	290
Fe	195	194	Fe	35	42
Mg	143	143	Mg	38	29
K	ND	ND	K	ND	ND
OC+EC	3731	3295	OC+EC	3905	4410
$CO_3^=$	1486	1374	$CO_3^=$	409	456
Na	537	592	Na	172	91
Cl	358	395	Cl	115	61
ss-$SO_4^=$	134	148	ss-$SO_4^=$	43	23
nss-$SO_4^=$	3836	4569	nss-$SO_4^=$	3691	4561
NO_3^-	1104	1094	NO_3^-	209	178
NH_4^+	878	1205	NH_4^+	1106	1507
Zn	30	49	Zn	40	12
Ti	19	25	Ti	6	4
P	36	34	P	3	24
Pb	6	5	Pb	5	0
Ba	5	57	Ba	23	4
Sr	4	4	Sr	1	1
Mn	4	4	Mn	2	1
Ni	3	7	Ni	3	16
Cu	55	14	Cu	30	21
V	4	2	V	3	1
Cr	1	2	Cr	1	1
N samples	3	3	N samples	3	3
Σcomponents	15882	16894	Σcomponents	10760	12154
Determined %	90	87	Determined %	84	89
Crustal	5199	5513	Crustal	1437	1270
Secondary	5818	6868	Secondary	5005	6246
OC+EC	3731	3295	OC+EC	3905	4410
Marine	1030	1135	Marine	330	175

Table 6-5.C). Mean diurnal and nocturnal major and trace elements and bulk PM10 levels (in ng/m^3) obtained in the period July 24-27 at MORELLA. N, number of samples. The source apportionment (in ng/m^3) of PM10 includes the crustal source, secondary particulates (ammonium sulphate and nitrate), organic+elemental carbon (OC+EC) and sea spray (Na +Cl+ss-$SO_4^=$).

July 24-27	C) MORELLA	
PM10	Night	daylight
	23:00-7:00	11:00-19:00
PM10.	16836	15787
Ca	646	493
Al_2O_3	471	686
SiO_2	1178	1714
Fe	197	193
Mg	101	135
K	ND	ND
CO+CE	2333	2717
$CO_3^=$	969	740
Na	402	601
Cl	268	400
ss-$SO_4^=$	100	150
nss-$SO_4^=$	2691	3899
NO_3^-	803	997
NH_4^+	1071	1285
Zn	ND	11
Ti	26	28
P	16	34
Pb	5	2
Ba		14
Sr	2	2
Mn	4	5
Ni	6	5
Cu	15	3
V	2	2
Cr	3	2
N samples	3	3
Σcomponents	11310	14119
Determined %	67	89
Crustal	3606	4038
Secondary	4566	6182
OC+EC	2333	2717
Marine	770	1151

5) levels of NH_4^+ in PM2.5 are higher than in PM10. This behaviour was also observed in the Barcelona Metropolitan Area and was attributed to the volatilisation of $ClNH_4(g)$ by the reaction of NH_4NO_3 with NaCl (details in section 5.2.3 in chapter 5).

Owing to the prevalence of advective conditions, PM10 and PM2.5 components did not show significant daily cycles in the period July 24 to 27 (Table 6-4).

6.2.5 Cascade impactor sampling

Figure 6-28 shows the size distribution of the soluble and insoluble fractions of major species in total suspended particles obtained at MONAGREGA from July 16 to 21 2000. Ammonium-sulphate is mainly concentrated in the finest fractions (0.4-0.7 and 0.7-1.5 µm, respectively). The <1.5µm fraction accounts for 60 % of the bulk anthropogenic sulphate. The coarser sulphate mostly occurs as calcium and sodium sulphate.

The marine aerosol phase is mainly concentrated in the 1.5-6 µm fraction as inferred from the Na distribution. The excess of Na with respect to Cl is attributed to the volatilisation of Cl caused by the reaction of acids with sea salt (Harrison and Pio, 1983; Wall et al., 1988; Pio and Lopes 1998), especially with nitric acid (HNO_3) and/or ammonium-nitrate (NH_4NO_3) as suggested by the occurrence of $NaNO_3$ in the cascade impactor (mainly in the 0.7-6 µm fraction). Sodium chloride mainly occurs in the >6µm fraction, whereas sodium nitrate in the <6 µm. The occurrence of NO_3^- in the >6 µm fraction is attributable to nitrification of Ca-rich soil particles to form $Ca(NO_3)_2$ (Harrison and Kito, 1990).

Nss-$SO_4^=$, NO_3^-, Cl^-, NH_4^+, Ca^{++}, Sr^{++}, Mg^{++}, Mn^{++} and Pb^{++} are mainly present in the soluble fraction, whereas Al, Zn, Fe and Ti mainly occur in the insoluble fraction. K, V and Ba were significantly present (~50%) in both soluble and insoluble fractions. Insoluble soil particulates such as clay minerals, calcium carbonate and feldspars (crustal phases) showed a bi-modal grain- size distribution with modes occurring in the 1.5-6.0 µm and >25 µm fractions as deduced from the grain-size distribution of insoluble levels of Ca, Al, K and Fe.

6.2.6 PM10 & PM2.5 during fumigations of the high SO_2-plume

Table 6-6 shows the levels of PM10 and PM2.5 components in samples collected in the SO_2 plume during impacts on the ground levels at noon and in the afternoon in the period July 19 and 20 2000. Levels of SO_2 and grain size distribution of PM were also continuously measured simultaneously with PM10 and PM2.5 sampling.

Most of nss-$SO_4^=$ during the SO_2 plume fumigation is neutralised (as ammonium-sulphate $(NH_4)_2SO_4$ and/or NH_4HSO_4), although there is a significant fraction of acidic nss-$SO_4^=$ (~25%; Figure 6-29). Note that the slope of the cross correlation of nss-$SO_4^=$ versus NH_4^+ levels during the SO_2 fumigations (1.25, see Figure 6-29) is significantly higher than in ambient air (1.08, see Figure 6-25A). This is attributed to the occurrence of recently formed sulphuric acid (H_2SO_4) in the SO_2 plume, which is progressively neutralised by ammonia during the ageing of the air mass. On July

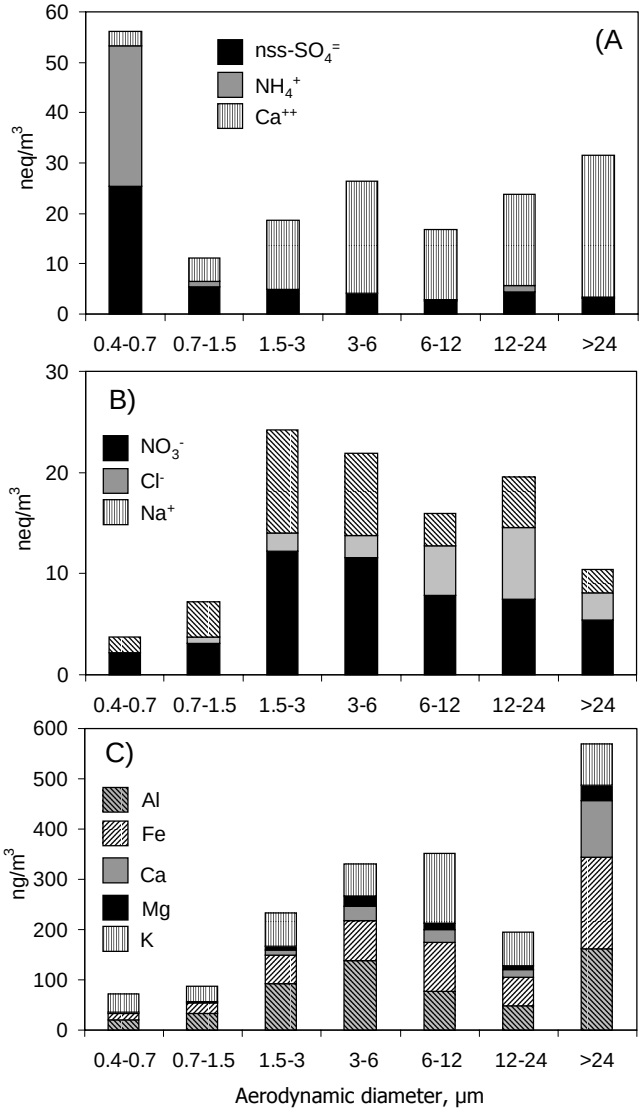

Figure 6-28. Grain-size distribution of the soluble (A and B in neq/m^3) and insoluble (C in ng/m^3) fractions of major species in total suspended particles obtained at MONAGREGA for July 16 to 21 2000.

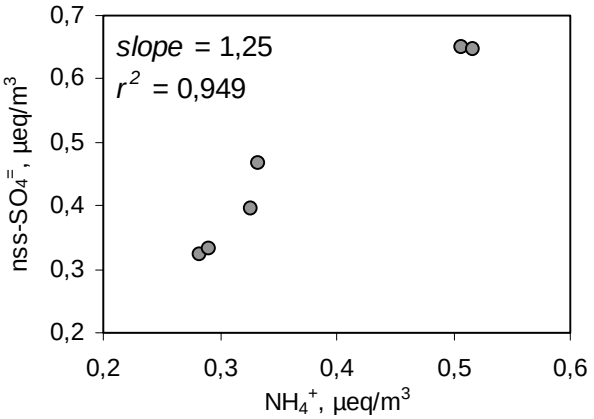

Figure 6-29. Cross correlation plot of nss-$SO_4^=$ versus ammonium levels in PM10 and PM2.5 samples taken during fumigations of the SO_2 plume (Table 2) on July 19 and 20 2000.

19 levels of nss-$SO_4^=$ recorded in the ambient air monitoring stations were in the range 6-10µg/m^3 whereas nss-$SO_4^=$ level in the SO_2 plume was 16µg/m^3. On July 20 levels of nss-$SO_4^=$ were in the range 20-30µg/m^3 in the SO_2 plume and in the range 14-21µg/m^3 in ambient air. Thus, nss-$SO_4^=$ levels in the SO_2 plume were 1.5 to 2.5 higher than those recorded in ambient air on July 19 and 1.5 higher than those recorded in ambient air on July 20. These "nss-$SO_4^=$ plume/nss-$SO_4^=$ ambient air" concentration ratios ranging between 1.5 and 2.5, are very low when compared with the "SO_2 during fumigations/SO_2 in ambient air" concentration ratios, which is frequently in the range 8 and 50 (see SO_2 levels frequently in the range <10-20µg/m^3 in ambient air and 80-1000µg/m^3 during SO_2 fumigations in Figures 6-24 and 6-30 respectively). These low nss-sulphate ratios indicate high background concentration of nss-$SO_4^=$ in the study area.

Owing to the fact that nss-sulphate occurs in the fine mode of PM, similar nss-$SO_4^=$ levels are recorded in PM2.5 and PM10. PM2.5 is mainly constituted by ammonium-sulphate and other anthropogenic species (e.g. OC+EC), whereas PM10 includes, in addition to the PM2.5 bearing species, components of crustal and marine origins. The only exception is NO_3^-, which is mainly in the 2.5-10µm fraction during daylight.

During the SO_2 fumigations, levels of PM1 showed a high degree of correlation with SO_2 levels (Figure 6-30) which is mainly attributed to the newly formed sulphate particles in the plume, as deduced from the PM2.5 and cascade impactor samples. In contrast, levels of PM10 did not show a significant correlation with SO_2 levels due to the fact that the 1-10µm fraction contains a large number of PM species not derived from the SO_2 plume (e.g. mineral dust). PM2.5 presents an intermediate behaviour between PM10 and PM1. PM1 is an adequate parameter for monitoring the impact of the SO_2 plume fumigations on the surface. Note that the 1-minute time series of PM10 is much noisier than that of PM1.

Table 6-6. Mean levels (in ng/m^3) of major and trace elements obtained in PM10 and PM2.5 samples collected during impacts of the SO_2-plume on the surface. The source apportionment (in ng/m^3) of PM10 includes the crustal source, secondary particulates (ammonium sulphate and nitrate), organic+elemental carbon (OC+EC) and sea spray (Na +Cl+ss-$SO_4^=$). Time presented as LST.

	Fumigation-1	Fumigation-1	Fumigation–2	Fumigation-2	Fumigation-3	Fumigation-3
	19/07/00 from: 14:54 to:18:51	19/07/00 from: 14:54 to: 18:51	20/07/00 from: 13:35 to: 15:20	20/07/00 from: 13:35 to: 15:20	20/07/00 from: 15:40 to: 19:04	20/07/00 from: 15:40 to: 19:04
	PM10	PM2.5	PM10	PM2.5	PM10	PM2.5
PM	51587	38600	85618	78291	55429	38455
Ca	1733	520	1890	616	1264	176
Al_2O_3	1465	426	1593	931	1277	199
SiO_2	3663	1064	3982	2328	3193	498
Fe	405	167	303	96	345	92
Mg	241	96	418	222	259	61
K	ND	ND	ND	ND	ND	ND
OC+EC	3880	4485	4398	8731	3707	3323
$CO_{3=}$	2600	780	2835	924	1897	265
Na	933	187	1726	962	1074	201
Cl	622	125	1151	642	716	134
ss-$SO_4^=$	233	47	432	241	268	50
nss-$SO_4^=$	15521	15936	31164	31059	22321	19005
NO_3^-	1399	79	971	39	1103	29
NH_4^+	5082	5243	9126	9319	6009	5887
Zn	153	49	273	300	119	28
Ti	33	13	37	36	32	5
P	61	114	97	114	80	37
Pb	ND	ND	34	19	ND	ND
Ba	141	2	321	339	118	3
Sr	8	2	13	7	7	1
Mn	7	4	12	5	9	3
Ni	7	<1	26	<1	<1	<1
Cu	ND	ND	ND	ND	ND	ND
V	3	<1	3	<1	<1	<1
Cr	2	<1	4	<1	4	2
Σmajor elem.	38174	29336	59932	56370	43789	29995
Determined%	74	76	70	72	79	78
Crustal	10504	3233	11763	5798	8590	1365
Secondary	22002	21259	41262	40417	29433	24920
OC+EC	3880	4485	4398	8731	3707	3323
Marine	1788	359	3309	1845	2058	386

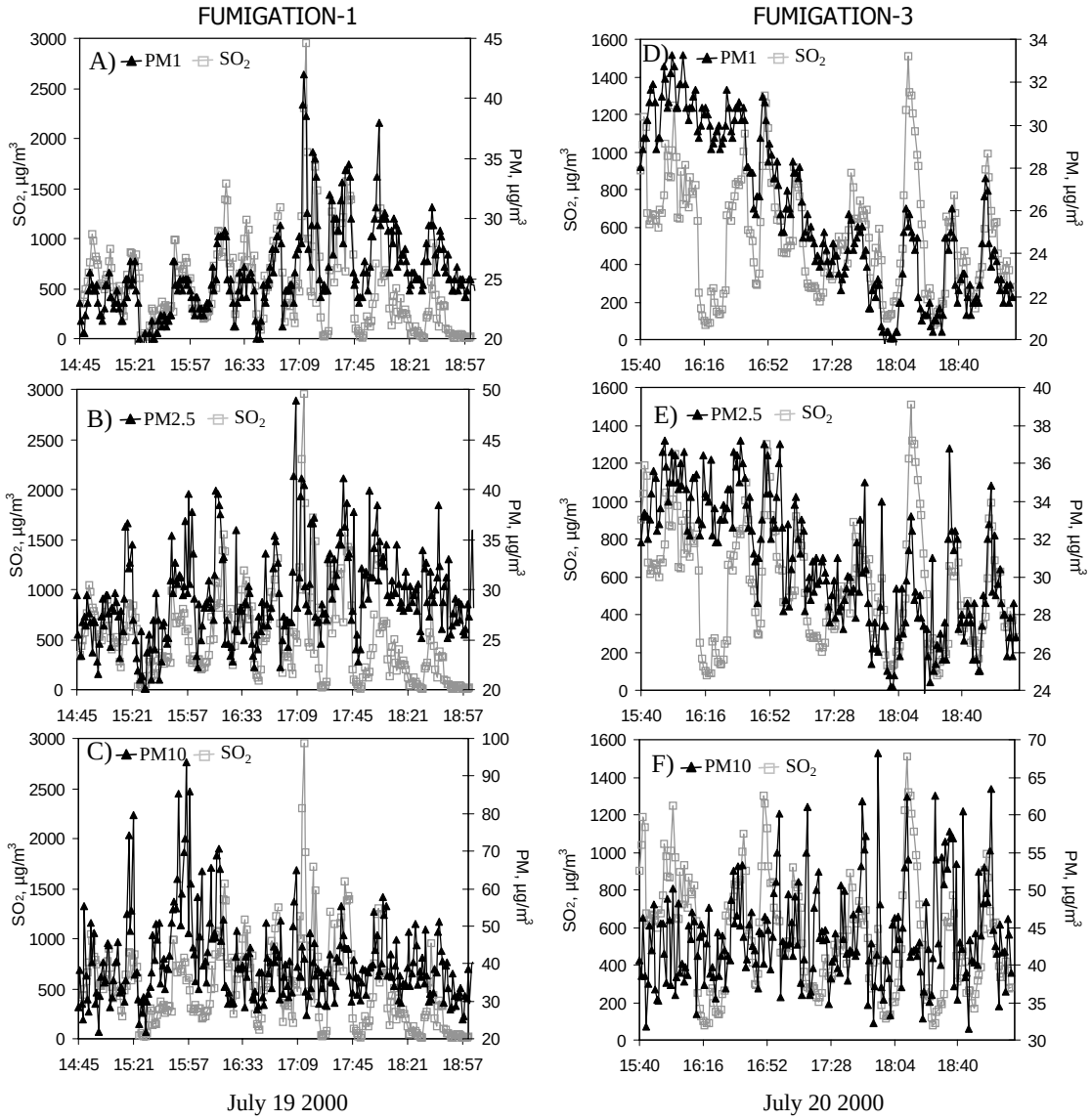

Figure 6-30. One-minute SO_2 PM10, PM2.5 and PM1 concentrations measured under the influence of the SO_2 plume of Teruel power plant during July 19 and 20 2000.

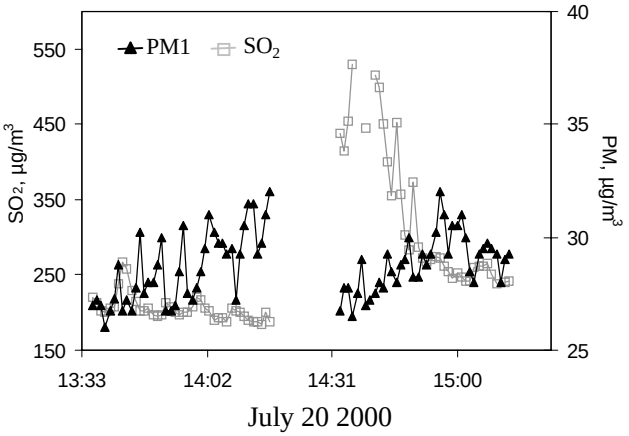

Figure 6-31. One-minute SO_2 and PM1 concentrations measured under the influence of the SO_2 plume of Teruel power plant on July 20 2000.

The high correlation between SO_2 and PM1 levels was not observed during the fumigation-2 (Figure 6-31). Moreover, a decrease in PM1 levels was recorded during the increase in SO_2 levels. This is probably due to fact that high PM1 and nss-sulphate (Figure 6-24) levels were recorded in ambient air due to the presence of aged polluted air. Under these conditions background levels of PM1 in ambient air were higher than under the influence of the high SO_2 fresh air mass.

6.2.7 Grain-size distribution of PM around sources and in ambient air

Figure 6-32 and Table 6-7 shows the grain size distribution of PM around several PM sources (see location in Table 6-2). The fumigations of the SO_2 plume on the surface led to very high levels of fine PM in such a way that almost all TSP was constituted by PM10 (70-85%wt) and a very important fraction of TSP was made up of PM2.5 (50-70%). PM10 presented high loads of PM2.5 (70-90%wt) and PM1 (40-50%wt). The grain size distribution of PM during the SO_2 fumigations present a maximum in the fraction <0.5µm, similar to that presented by nss-$SO_4^=$ in the cascade impactor. An opposite grain size distribution was obtained in the areas affected by soil dust re-suspension driven by wind over semi-arid soils or coal piles (at the Teruel power station), or by crop cultivation, grazing and mining. The PM10 load in TSP ranged in the interval 30-35%wt at the sites affected by crop cultivation, mining and arid soils, and in the range 12-20%wt in the sites affected by grazing and re-suspension on the coal piles. The load of PM2.5 in TSP was ~12%wt at the semi-arid soil site and ≤5%wt at the other sites. The load of PM2.5 and PM1 in PM10 was ~40 and 20%wt at the semi-arid soil site and ranged in the intervals 8-15 and 4-5 %wt, respectively. The higher PM2.5 and PM1 loads in PM10 at the semi-arid soil site (natural re-suspension), is probably due to the lower PM emissions (around one order of magnitude lower, see Table 6-7 and Figure 6-32) than at the sites affected by anthropogenically forced re-suspension. A

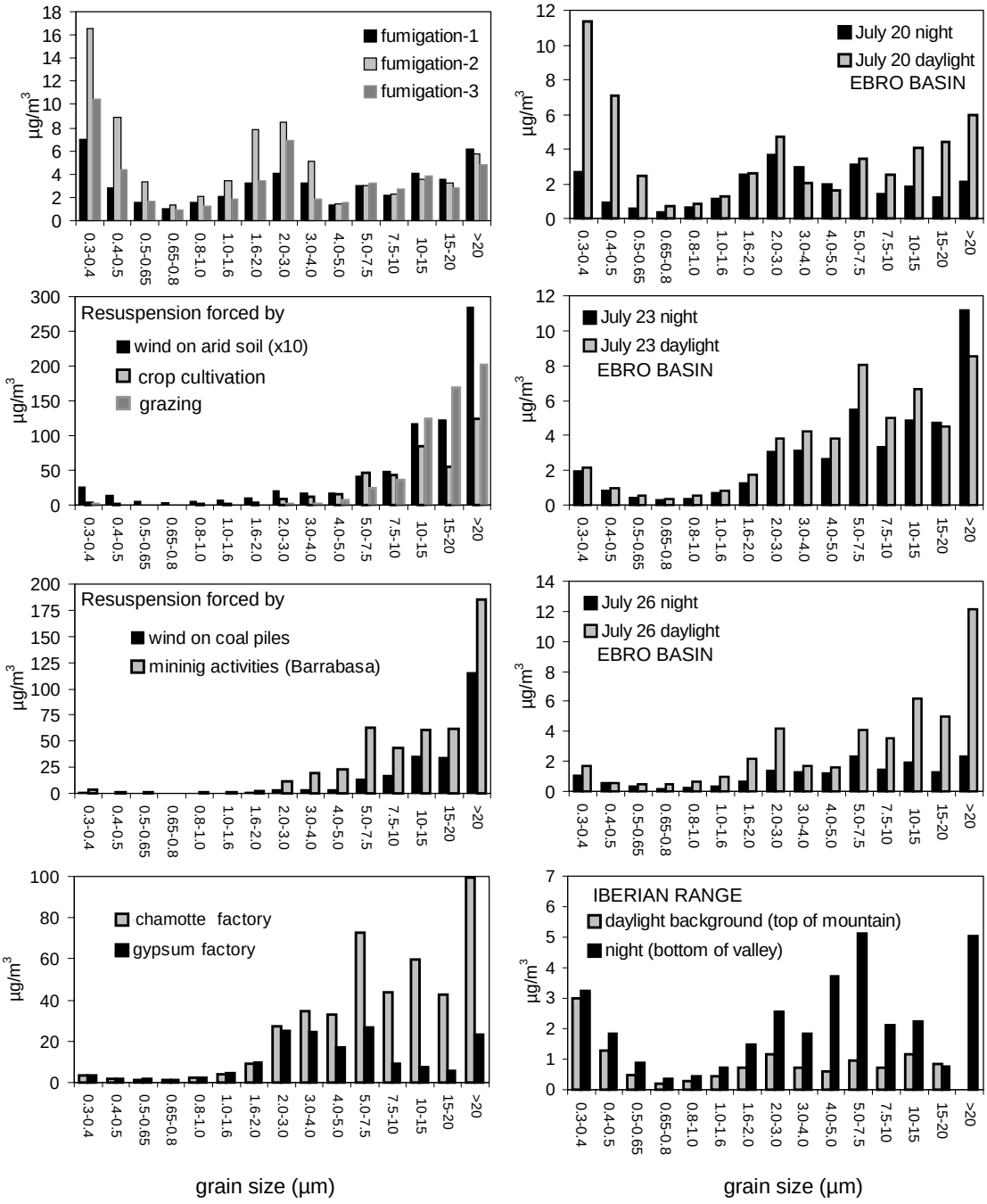

Figure 6-32. Grain size distribution of PM around several PM sources (left column) and in ambient air (right column).

Table 6-7. Levels of PM in different grain size cut off around several PM sources and in ambient air. IBR: Iberian/Catalan range, EB: Ebro basin. Backg: background. See location in Figure 6-18.

		TSP	PM10	PM7.5	PM5	PM2.5	PM1.0	PM0.8
PM source emissions								
Fumigations of SO_2								
Fumigation-1	E-1a	47	33	31	28	23	14	12
Fumigation-2	E-1b	76	64	62	59	56	35	30
Fumigation-3	E-1c	52	40	38	34	31	19	18
Re-suspension forced by								
wind on arid soil	E-2	74	22	17	12	9	5	5
crop cultivation	E-3	401	138	95	48	21	7	7
grazing	E-4	571	76	39	15	6	3	3
wind on coal piles	E-5	228	44	27	13	6	2	1
mining	E-6	477	170	127	64	22	7	6
Other Sources								
chamotte factory	E-7	435	234	190	118	50	10	8
gypsum factory	E-8	164	127	118	91	50	10	8
Ambient air measurements at background sites								
EB daylight July 20	A-2	55	41	38	35	33	22	22
EB daylight July 22	A-3	54	35	29	20	16	4	4
EB daylight July 23	A-3	52	32	27	19	14	5	4
EB daylight July 26	A-3	46	22	19	15	12	4	3
EB night July 19	A-3	46	33	30	24	18	9	8
EB night July 20	A-3	27	22	20	17	14	5	5
EB night July 22	A-3	56	39	33	22	16	3	3
EB night July 23	A-3	44	23	20	15	11	4	3
EB night July 24	A-3	26	16	14	10	8	3	2
EB night July 25	A-3	33	22	19	14	11	4	4
EB night July 26	A-3	16	11	9	7	6	2	2
EB night July 27	A-3	41	27	24	18	16	5	5
IBR (top) daylight July 18	A-1	13	11	10	9	8	5	5
IBR (valley) night July 21	A-4	32	24	22	17	12	7	6

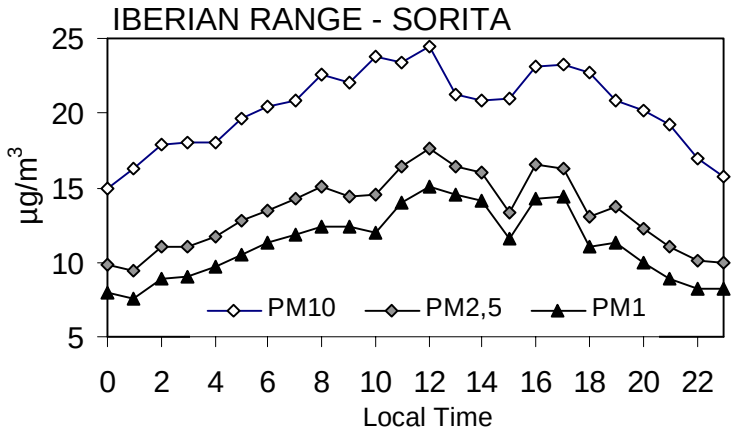

Figure 6-33. Hourly averaged PM10, PM2.5 and PM1 levels in the period 16-21 July 2000 at SORITA station.

significant fraction of the fine PM over the semi-arid soils is probably caused by the background concentrations of nss-$SO_4^=$ in the study area. PM grain size distribution was also measured around a gypsum and chamotte factory. A relatively high PM10 fraction in TSP was observed in the gypsum factory emissions, induced by a mode in the PM size range 3.0-7.5µm (Figure 14), probably by milling processes in the gypsum production. Notice that TSP and PM10 levels at the sites affected by natural or anthropogenically forced soil dust re-suspension are much higher than at the sites affected by the SO_2 plume fumigations (Table 6-7).

Measurements of PM grain size distribution were also performed in ambient air at sites outside local PM sources (rural and background sites, Figure 6-32 and Table 6-7, see location in Table 6-2). In the Ebro basin (MONAGREGA station), the load of PM10 in TSP was mostly in the range 60-75%wt. The PM10/TSP ratio underwent a daily cycle characterised by higher values at night than during daytime owing to the re-suspension of crustal PM >10µm during daylight (see July 20, 22, 23 and Table 6-7 and Figures 6-28 and 6-32). The load of PM2.5 and PM1 in PM10 mostly ranged in the interval 40-70 and 10-20%wt, respectively. An exceptionally high PM2.5/PM10 (=80%wt) and PM1/PM10 (=54%wt) ratios episode was recorded during daylight on July 20 owing to the extremely high nss-$SO_4^=$ concentrations (Figure 6-24). This is evident in the grain size distribution of PM, which showed a maximum in the <0.5µm grain size (Figure 6-32). The grain size distribution of PM at the Ebro basin tends to present three modes, in the range of sizes <0.5µm, 1.6-4.0µm and >5.0µm. In accordance with the cascade impactor sampling, the mode <0.5µm is interpreted as caused by ammonium-sulphate. The mode in the range 1.6-4.0µm is correlated with the grain size distribution of soluble Na, Ca and NO_3^- (probably as a result of the interaction of nitrogenous gases or particulates with Ca from soil or marine Na) and some crustal insoluble species (Al and Fe), probably occurring as clay minerals. Finally, the mode >5.0µm is mainly constituted by crustal PM.

The nocturnal grain size distribution of PM in the Iberian range (SORITA station) was very similar to that recorded in the Ebro basin (Figure 6-32 and Table 6-7). However, the grain size distribution under background conditions at the top of the Iberian range during daylight was very different from that recorded at the Ebro basin since it presented a maximum in the range size <0.5μm (Figure 6-32 and Table 6-7). Very low PM levels were recorded at this site in the Iberian range because the measurements were performed at the end of an Atlantic episode (which cleaned the atmosphere) and because the measurement site was surrounded by a Mediterranean forest which inhibited the re-suspension of coarse PM.

In the Iberian range (SORITA station) the load of PM2.5 and PM1 in PM10 was mostly in the range 65-80%wt. A lower load of crustal PM in the Iberian range accounts for the higher PM2.5 and PM1 load in PM10 in the Iberian range than in the Ebro basin (as demonstrated by the chemical composition, Table 6-4).

Figure 6-33 shows hourly levels of PM10, PM2.5 and PM1 (averaged from July 16 to 21) in the Iberian range. It should be noted that the previously described daily cycles affect the three fractions of PM.

6.3 PM characterisation around primary particulate anthropogenic emissions

6.3.1 The study area

The industrial area of ceramic production located at L'Alcora, Onda and Vila-real spread along the Millars river basin from the coast to the interior of the Castelló Province in Eastern Spain (Figure 6-34). The Castelló industrial area is the second largest centre for the manufacture of ceramics in the world, accounting for 17 % of the world's production ($600x10^6$ m^2/year). The supply of clays for the industry comes mainly from an open-pit mine at a Triassic red kaolinite-rich clay deposit in Sant Joan de Moró (east of the city of L'Alcora, Figure 6-34) and from the Cretaceous kaolinite-rich deposits in the province of Teruel. A wide variety of other natural and synthetic products such as feldspars, melting phases and colourants are also broadly employed, but to a lesser extent than clay consumption. The kaolinite-rich material is finely ground in the atomisers which produce an homogeneous fine powder (<63 μm). This process coupled with the large clay consumption ($20x10^6$ tonnes in 1998) and the large fugitive emissions from the storage, handling and transport of the clay, probably account for the largest fraction of the local anthropogenic particulate emissions.

Secondary particulate emissions from the manufacturing of glass and enamel may account more for the emission of hazardous atmospheric trace pollutants than for their significant contribution to the bulk particulate emissions. Other particulate emission sources such as intensive road transport, frequent biomass combustion of orange tree wastes and marine aerosols are also considered.

These particulate-emissions occur in the complex atmospheric environment in the Western Mediterranean. The intensive convective dynamics, the breeze circulation, the low rainfall rate and the highly mineralised soils further complicate the monitoring of the impact of the anthropogenic particulate emissions on ambient air quality. This study was carried out in July because of the large impact of some of the aforementioned atmospheric environmental factors on the particulate levels.

The study area (Figure 6-34) includes the Castelló alluvial plain (La Plana), which is bounded on the north by the Palmes mountain chain (6-7 Km from the coast), and includes Mt. Bartolo as its highest peak (780 m.a.s.l.). The Millars basin, which has an approximate E-W direction, converges on the first range of mountains at 20 Km from the coast.

The movement of the air masses over the eastern coast of the Iberian Peninsula as well as the evolution of the boundary layer are strongly linked to its complex topography. During the daytime the sea breeze is channelled along the bottom of the valleys up to 60-80 km inland, whereas at the top of the mountains and valley-slopes a combination of sea breeze and up-slope winds gives rise to a chimney effect, injecting air from low levels to altitudes ranging from a few hundred meters up to 2-3 km (Millán et al., 1992). The anticyclonic subsidence and the dynamics development of the sea breeze cells favour the formation of reservoir layers of secondary pollutants (thermally separated by inversions) in the return flow moving toward the Mediterranean sea (Soriano et al., 2001). A compensatory sinking over the sea due to thermal buoyancy over the warmed terrain and anticyclonic subsidence reinforces the sea-breeze circulation and prepares the

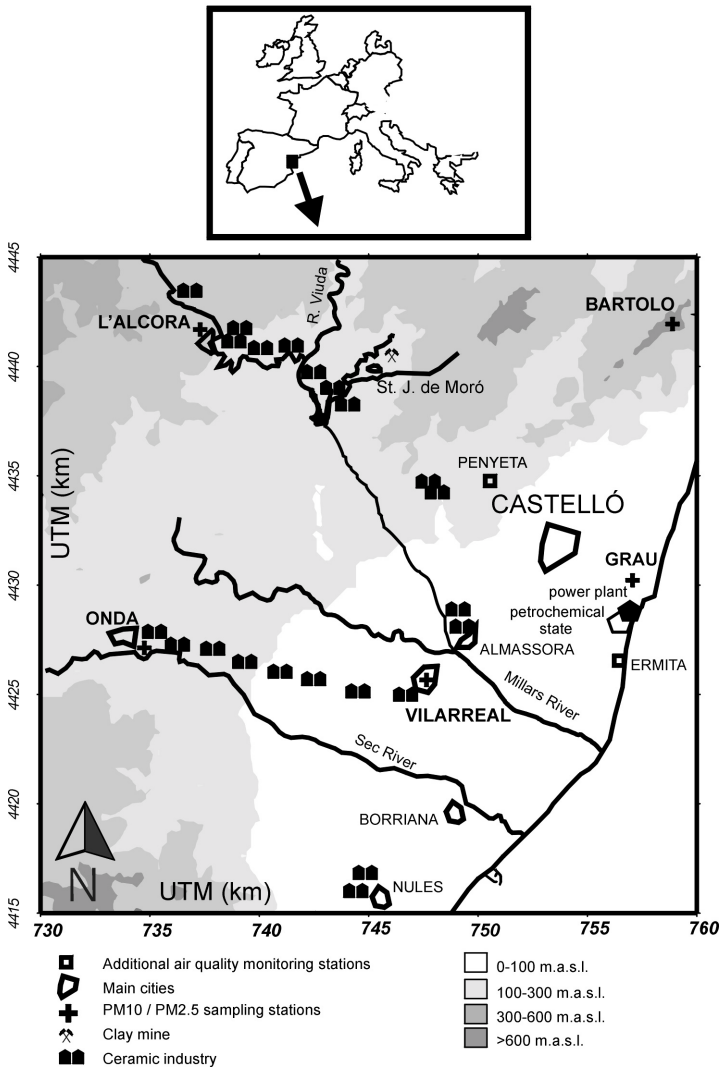

Figure 6-34. Location of major ceramic production areas and fixed sampling stations for PM10 and PM2.5 measurements.

reservoir layers over the sea for re-entrance a few days later. During the evening and night, the solar-activated circulations cease, and a reversal in the breeze takes place.

During the measurement campaign typical summer meteorological conditions predominated with a local-circulation dominance in the measuring zone despite the fact that a smooth perturbation aloft took place at the end of the first week. Thus, inland airflow during daytime and seaward airflow during night was the scenario that was daily repeated during the measurement campaign. The typical summer thermal vertical structure with subsidence inversions was also observed.

Table 6-8. Location of the fixed monitoring and sampling stations.

Sampling site	Location	Latitude	Longitude
Mt. BARTOLO	Telecom antenna peak	40º 05′ 09″N	00º 01′ 53″W
ONDA	Monitoring station (urban background station)	39º 57′ 43″N	00º 15′ 43″W
VILA-REAL	Post office (urban background station)	39º 56′ 34″N	00º 06′ 25″W
GRAU	Monitoring station (urban background station)	39º 58′ 59″N	00º 00′ 31″W
L'ALCORA	Council house (urban background station)	40º 05′ 09″N	00º 01′ 53″W

6.3.2 Sampling and measurements

The following sampling and measurement sites (Figure 6-34 and Table 6-8) were based on the distribution of the major emission sources (marine, rural, urban and industrial sites) and on the atmospheric-circulation peculiarities of the study area:

The GRAU station is located in a rural or semi-urban area which is sporadically influenced by industrial and urban plumes, especially the plume from Castelló during the nocturnal breeze period.

The station at VILLA-REAL is an urban site in the lower reaches of the river Millars, situated 10 km from the coastline, in the centre of the ceramic production zone. This station is influenced by both urban (mainly traffic) and industrial emissions. During the daytime period this location is situated leeward of the city and the ceramic emissions with respect to the characteristic breeze flow. For this reason, the contributions from traffic emissions should be equal or more important than those from industry. On the other hand, the ceramic emissions are expected to predominate during the nocturnal breeze period.

The ONDA station is a sub-urban background station near the town of ONDA, situated in an open area, 20 km from the coastline, without any direct influence from urban or road traffic activities. It is situated leeward of the nearby ceramic industries, and in the sea-breeze period it is also influenced by coastal industrial/urban emissions.

The L'ALCORA station is located at an urban background site in the municipality of L'Alcora in the most productive area of ceramic manufacture in Castelló. In the daytime the breeze drags the atmospheric emissions with a North-western transport, whereas during the nocturnal breeze period the previously emitted particulates travel seawards towards L'Alcora.

The BARTOLO station is located at the top of Mt. Bartolo. Possible anthropogenic emissions could come from a nearby residential area and from various roadways concentrated on the coastal fringe. The aim of using this emplacement was to provide a vertical gradient for discriminating possible high altitude contributions not present at lower levels.

Meteorological data from the air quality network stations at Ermita and Penyeta and from the meteorological towers at Cirat, Rambla de la Viuda and Borriana were also interpreted.

The sampling of atmospheric particulate matter was carried out by means of high volume samplers (DH-80 and MCV-CAF, 30m^3/h) equipped with PM10 and PM2.5 DIGITEL and MCV cut-off inlets and quartz glass filters (QF20 Schleicher and Schuell). Daily sampling was made from 12-23 July 1999 at the five fixed monitoring stations (Table 6-8). Furthermore, sampling of TSP grain-size

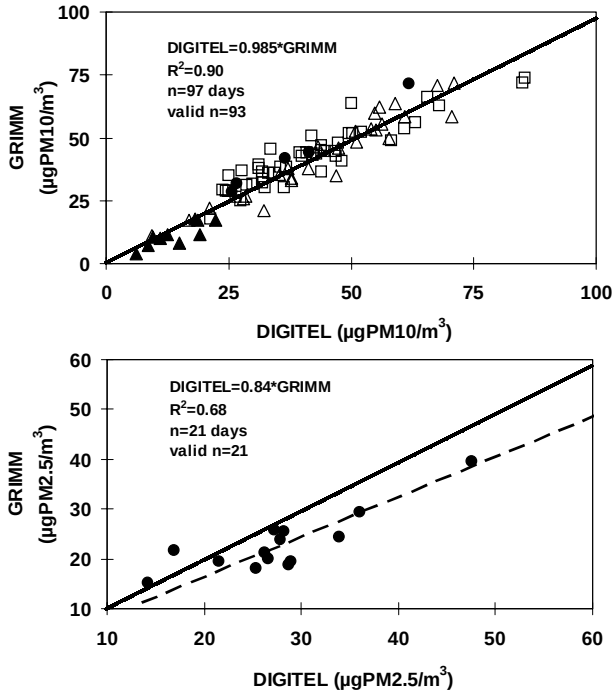

Figure 6-35. Correlation of PM10 and PM2.5 measurements between the GRIMM laser spectrometer and the high-volume sampler. Solid lines indicate 1:1, dashed line is the correlation line. In PM10, correlation was performed at the following sites: 1. Solid circles, sub-urban ONDA station; 2. Solid triangles, rural Monagrega station; 3. Triangles, urban Barcelona station, 4. Squares, urban L'HOSPITALET station. PM2.5 correlation was performed at ONDA (2 samples) and L'HOSPITALET.

fractions (7 stages from 0.3 to >20µm) was performed for 4 days (from 11-23 July 1999) at the ONDA station by means of a Retsch PI-1 cascade impactor.

Levels of bulk particulates were obtained by weighing the filters using standard procedures. Filters and cascade impactor samples were chemically analysed to determine levels of major and trace species in accordance with the procedures described in chapter 3.

Automatic measurements of atmospheric particulate levels and grain-size distribution were performed with the laser spectrometer dust monitor GRIMM 1108 (Labortechnik GmbH & Co. KG) at the fixed and mobile stations. This dust monitor permits the determination of particulate levels in 15 different grain-size channels in the range 0.3 to >20 µm. The accuracy of the GRIMM-1108 measurements was checked before, during and after the field campaigns by comparing the levels of simultaneous daily PM10 and PM2.5 measurements using standard gravimetric methods. Figure 6-35 shows good agreement between the PM10 measurements obtained with the high volume sampler and the GRIMM-1108 laser spectrometer. Although good agreement is also achieved in the two simultaneous PM2.5 measurements during the field campaign, a longer inter-comparison demonstrated that the GRIMM 1108 measurements are 15 % lower than those using the gravimetric method (Figure 6-35).

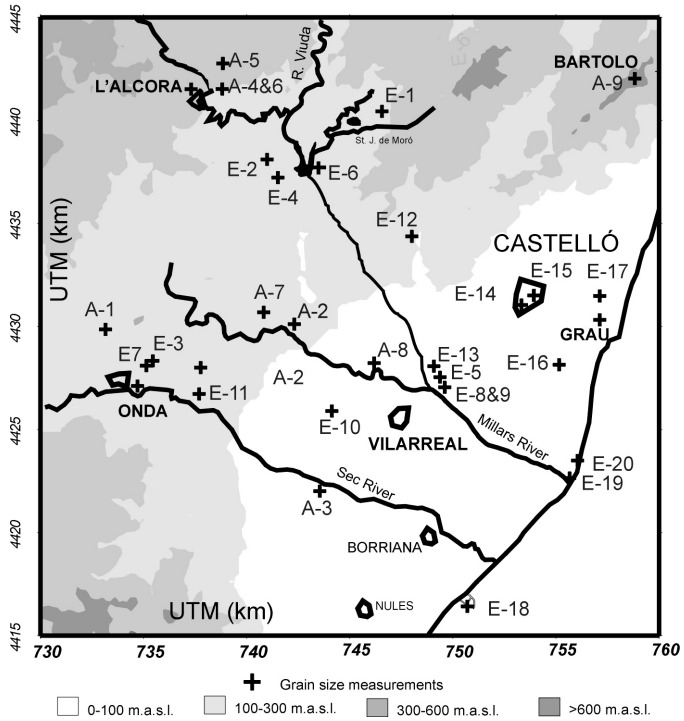

Figure 6-36. Location of mobile measurement stations for grain-size analysis of TSP with the GRIMM laser spectrometer around the major emission sources (E) and ambient air measurements (A). See detailed data of location in Table 6-9.

The measurements of particulate-matter levels and grain-size distribution with the laser spectrometer were carried out in the vicinities of the following emission sources (Table 6-9 and Figure 6-36):

1. Different types of ceramic emission plumes including those from enamel (white to yellow plumes) and tile (reddish plumes) factories and atomiser centres. Fugitive emissions were measured at a given distance from a number of sources including the stockpiles at the atomiser centres, the largest open-pit mine in the area, and a crossroads where high emissions from the short road transport between the clay-mining area and the tiling and atomising centres were evident.

2. The traffic emissions in the vicinity of a crossroads with high traffic density (mainly cars) at two different sites inside the city of Castelló.

3. The marine aerosol at three different coastal sites (a few metres from the shoreline) in the inland breeze circulation stage.

4. The biomass combustion emissions were measured at different distances from the fires in extensive orange-tree plantations located upwind from the ceramic emissions in the GRAU area.

Table 6-9. Location of mobile station for grain-size analysis of TSP with the GRIMM laser spectrometer around the major emission sources (E) and ambient air measurements (A).

N°	Measurement description	Longitude	Latitude
E-1	Fugitive emissions from a clay mine	00º06'31"W	40º04'39"N
E-2	Fugitive emissions from clay transport at L'Alcora	00º10'08"W	40º03'00"N
E-3	Atomiser, ONDA	00º14'35"W	39º58'18"N
E-4	Atomiser L'Alcora	00º10'29"W	40º03'29"N
E-4b	Atomiser L'Alcora second measurement	00º10'29"W	40º03'29"N
E-5	Around stack emissions PA factory	00º04'50"W	39º57'38"N
E-6	Around stack emissions SA factory	00º09'11"W	40º02'36"N
E-7	Around stack emissions VE factory	00º14'49"W	39º58'11"N
E-8	Around stack emissions JM factory	00º04'21"W	39º57'51"N
E-9	Around stack emissions JM factory 2nd measure	00º04'20"W	39º57'56"N
E-10	Around stack emissions EG factory	00º09'35"W	39º56'41"N
E-11	Around stack emissions NA factory	00º13'07"W	39º57'41"N
E-12	Around stack emissions POR factory	00º05'38"W	40º01'21"N
E-12b	Emission plume measurement POR factory	00º05'38"W	40º01'21"N
E-13	Emission plume measurement PA factory	00º04'41"W	39º57'22"N
E-14	Dense traffic crossroads at Castelló	00º02'14"W	39º59'22"N
E-15	Dense traffic crossroads at Castelló	00º03'19"W	39º58'19"N
E-16	Emission plume from petrochemical plant	00º01'06"W	39º57'06"N
E-17	Biomass fires around orange tree plantations	00º01'03"W	39º59'36"N
E-18	Marine aerosols Borriana harbour (Morro)	00º04'13"W	39º51'32"N
E-19	Marine aerosols Millars delta	00º00'49"W	39º54'22"N
E-20	Marine aerosols Ben Afali beach	00º00'15"W	39º55'20"N
E-20b	Marine aerosols Ben Afali beach on the shoreline	00º00'15"W	39º55'20"N
A-1	Northern background levels around the ceramic zone	00º16'10"W	39º59'10"N
A-2	Middle background levels in orange plantations	00º09'44"W	39º59'09"N
A-3	Coastal background levels leeward of ceramic emissions	00º04'03"W	39º54'45"N
A-4	Urban background levels L'Alcora	00º11'20"W	40º04'02"N
A-5	Semi-urban background levels L'Alcora (St Salvador)	00º11'49"W	40º05'11"N
A-6	Urban background levels L'Alcora	00º12'30"W	40º04'10"N
A-7	Semi-urban background levels L'Alcora – ONDA	00º10'46"W	39º59'29"N
A-8	Semi-urban background levels Millars bridge	00º07'11"W	39º57'54"N
A-9	Rural-remote background levels Mt. Bartolo	00º01'53"W	40º05'09"N

5. The emission plume from the petrochemical plant was detected with the help of the SO_2 analysers in a COSPEC unit and, subsequently, grain-size measurements were obtained without interference of the ceramic emissions in the in-land breeze stage.

In addition to the emission measurements, short (1-to-2 hour) measurements were performed in background areas up- and down-wind of the emission plumes from the areas of ceramic manufacture (Table 6-9 and Figure 6-36). The measurements were performed in the in-land breeze stage following a cross-section from the shoreline (backwards to the petrochemical and ceramic emissions), downwind of the petrochemical emission and finally downwind of the ceramic emission plumes. Short measurements were also carried out at different background sites influenced by different ceramic emission sources.

Longer measurements (24 hours) were carried out at the GRAU, L'ALCORA and ONDA stations to study the grain size range of atmospheric particulates influenced by the ceramic emissions transported by the breeze circulation.

6.3.3 PM10 & PM2.5 levels

As might be expected, the lowest PM10 mean values were obtained at the Mt. BARTOLO background station (18 µg/m^3). The highest PM10 values are registered at the L'ALCORA and VILA-REAL stations (56 and 44 µg/m^3, respectively) which are located in the most important areas of ceramic manufacture. The GRAU and ONDA stations, located in rural or sub-urban areas which are temporarily influenced by the emission plumes, have intermediate PM10 values of approx 30 µg/m^3. The mean PM2.5 fraction of PM10 in the study area is approx 50 %wt, whereas the mean PM10 fraction of total suspended particles (TSP) is approx 65 %, with extreme mean daily values from 50 to 80 %wt.

The levels of marine aerosols are homogeneously distributed in the study area as deduced from the narrow variations in the concentrations of Na^+, Cl^- and Mg^{2+} observed among the different sampling sites (Table 6-10). A similar homogeneous pattern is observed for levels of sulphate and ammonium (Table 6-10). The background, the sub-urban and the industrial stations show mean levels ranging only from 7 to 9 µg/m3 for anthropogenic sulphate and 2.1 to 2.8 µg/m3 for ammonium. The ionic balance between ammonium and sulphate demonstrates that around 80 % of the anthropogenic sulphate is present as ammonium sulphate. The occurrence of ammonium sulphate, sodium chloride and magnesium in discrete background aerosols accounts for the homogeneous levels of these phases in PM10 across the study area.

Conversely, the nitrate levels are considerably higher at the VILA-REAL site (with the highest traffic density) and lower, by a factor of 4 to 5, at the rural background site of Mt. BARTOLO (Table 6-10). A similar pattern is also observed for the distribution of levels of organic carbon and phosphorus. The other stations register intermediate values for nitrate and organic carbon with the exception of the sub-urban GRAU station. The frequent uncontrolled biomass combustion from intensive orange tree cropping around this station probably accounts for the high

Table 6-10. Daily mean levels (in ng/m^3) of major elements in PM10 and bulk PM10 levels obtained at Mt. BARTOLO, GRAU, ONDA, VILA-REAL and L'ALCORA sampling sites. N, number of daily samples. The source apportionment (in ng/m^3) include crustal sources, secondary particulates (ammonium, sulphate and nitrate), organic+elemental carbon (OC+EC) and sea spray (Na, Cl + ss-$SO_4^=$).

	BARTOLO	GRAU	ONDA	VILA-REAL	L'ALCORA
PM10	19523	36245	32125	44021	56047
Ca	514	1341	988	2315	2905
Al_2O_3	415	1125	1402	2414	4815
SiO_2	1156	2731	3609	6056	12017
Fe	219	421	421	704	1222
Mg	205	313	205	405	402
K	231	491	509	800	1515
OC+EC	2915	6122	3908	6800	5523
$CO_3^=$	720	1877	1383	3241	4067
Na	780	1201	978	1405	895
Cl^-	198	805	404	974	505
ss-$SO_4^=$	195	300	245	351	224
nss-$SO_4^=$	7352	8405	8695	8956	8395
NO_3^-	923	2910	1784	3505	1785
NH_4^+	1945	2556	2295	2119	1910
N samples	5	9	11	9	2
Σmajor elements	17768	30599	26826	40045	46180
Determined %	91	85	85	94	86
Crustal	3460	8299	8517	15935	26943
Secondary	10220	13871	12774	14580	12090
OC+EC	2915	6122	3908	6800	5523
Sea spray	1173	2306	1626	2730	1624

Table 6-11. Daily mean levels (in ng/m^3) of trace element in PM10 obtained at Mt. BARTOLO, GRAU, ONDA, VILA-REAL and L'ALCORA sampling sites. N, number of daily samples.

	BARTOLO	GRAU	ONDA	VILA-REAL	L'ALCORA
As	1	5	8	11	25
Ba	1	11	6	16	21
Cd	0,1	0,7	0,4	0,6	0,9
Co	0,4	0,3	0,6	0,6	1,1
Cr	0,6	1,7	2,2	3,6	6,9
Cs	0,1	0,3	0,4	0,5	1,2
Cu	77	36	6	39	88
Ga	0,1	0,1	0,2	0,2	0,5
Hf	0,2	0,4	0,4	0,5	0,4
Mn	5	7	7	11	13
Mo	0,6	0,6	0,8	2,9	2,2
Nb	0,1	0,1	0,1	0,2	0,3
Ni	5	3	4	7	9
P	15	50	32	52	42
Pb	45	199	285	346	341
Rb	1	1	2	3	6
Sb	1	2	1	2	2
Sc	0,1	0,1	0,1	0,2	0,3
Sn	1	2	1	2	2
Sr	2	4	4	6	10
Th	0,7	0,6	0,2	0,9	0,2
Ti	12	29	34	65	111
U	<0,1	0,2	0,6	<0,1	<0,1
V	8	7	7	10	14
Y	0,1	0,2	0,1	0,3	0,4
Zn	54	132	178	264	699
Zr	3	8	11	12	21
La	0,2	0,3	0,4	0,6	1,1
Ce	0,2	0,7	0,9	1,3	2,2
Tb	0,03	0,03	0,03	0,03	0,03
Tm	0,03	0,03	0,02	0,03	0,02
Yb	0,02	0,04	0,05	0,04	0,06
N samples	5	9	11	9	2

Table 6-12. Comparison between levels (in ng/m^3) of major and trace elements in PM10 and PM2.5 samples simultaneously collected at ONDA on July 21 (left column) and 22 (right column) 1999. The source apportionment (in ng/m3) includes crustal sources, secondary particulates (ammonium sulphate and nitrate), organic+elemental carbon (OC+EC) and sea spray (Na +Cl+ss-$SO_4^=$).

	PM10	**PM2.5**	**PM10**	**PM2.5**
PM10/PM2.5	33221	23198	37010	17098
Major elements				
Ca	1412	809	1401	215
Al_2O_3	1998	1201	2105	521
SiO_2	5125	2305	4923	710
Fe	489	305	602	203
Mg	301	98	305	95
K	603	510	685	390
OC+EC	2105	1205	2225	405
$CO_3^=$	4605	4410	5690	4611
Na	802	295	802	193
Cl^-	305	189	480	185
ss-$SO_4^=$	205	99	195	98
nss- $SO_4^=$	6795	6098	7085	6691
NO_3^-	1310	495	1384	425
NH_4^+	1915	1841	2124	2045
Σmajor elements	27970	19860	30006	16787
Determined %	87	90	84	100
crustal	43	33	41	16
secondary	36	42	35	54
OC+EC	16	22	19	27
Sea spray	5	3	5	3
Trace elements				
As	10	10	10	7
Ba	8	3	9	2
Cd	0.6	0.5	0.6	0.4
Co	0.5	0.2	0.5	0.1
Cr	2.0	1.5	2.1	1.0
Cs	0.5	0.4	0.5	0.3
Cu	10	9	10	10
Hf	0.3	0.1	0.1	0.3
Mn	7	5	8	3
Mo	0.3	0.2	<0.1	<0.1
Nb	0.2	0.1	0.2	0.1
Ni	3	3	3	3
P	33	22	32	12
Pb	354	330	368	245
Rb	3	2	3	1
Sb	1	1	1	1
Sn	1	1	1	1
Sr	5	2	6	1
Th	<0.1	<0.1	0.5	<0.1
Ti	48	28	51	14
U	<0.1	<0.1	<0.1	<0.1
V	6	5	7	7
Zn	197	186	204	170
Zr	8	4	8	5

levels of organic carbon, phosphorus and nitrate, similar to those recorded at the heavily polluted VILA-REAL site.

The levels of the major elements emitted by the ceramic industry (clay-related elements such as Si, Al, Fe, K and Ti) are one order of magnitude higher at the L'ALCORA and VILA-REAL stations than at the BARTOLO site, with the ONDA and GRAU stations having intermediate levels (Table 6-10). Levels of Ca and Mg, mainly derived from soil emissions with a low proportion from the ceramic industry, also increase in the ceramic zone with respect to those at the background site. However, this increase is less than that experienced by the ceramic related elements.

On an average, the addition of all the constituents determined reached 90 % of the bulk PM10 or PM2.5 levels obtained by the gravimetric method. The results indicate that the mean marine aerosol input represents between 3 (VILA-REAL) and 8 (GRAU) % wt of the bulk PM10 levels (Table 6-10). The proportion of organic and elemental carbon, mainly proceeding from combustion processes, is relatively homogeneously distributed across the study area with values from 12 to 20 % wt of bulk PM10, with the highest values being recorded for the GRAU and VILA-REAL sites (Table 6-10). The PM10 proportion from the crustal input (both soil and ceramic emissions) ranges from 18 % of bulk PM10 at the Bartolo site, up to 40 to 55 % wt in the ceramic production area. The ONDA and GRAU sites have intermediate proportions (around 30 %wt). Finally, the proportion of secondary inorganic aerosols (ammonium, sulphate and nitrate) is very high at the background site (near by 60 % of bulk PM10 levels) and the ONDA and GRAU sites (45 to 50 %wt), whereas in the ceramic zone (VILA-REAL and L'ALCORA) it is much lower (approx 30 %wt). This demonstrates the background level of ammonium sulphate in the study area. Thus, at the rural background site, these external phases account for most of the particulate fraction, whereas this proportion is drastically reduced in the ceramic zone, where the local input predominates.

Levels of Pb and Zn also reach relatively high values in the ceramic zone (around 0.4 $\mu g/m^3$, lower than the EU annual limit value stabilised in 0.5µgPb/m_3) but very low levels at the rural background site (0.05 $\mu g/m^3$, Table 6-11). Although the levels of the other elements are relatively low, with the exception of As (up to 25 ng/m^3) and Cr (up to 7 ng/m^3) at L'ALCORA and VILA-REAL, the spatial variation of levels of As, Cr, Cs, Pb, Rb, Sr, Ti, V, Zn and Zr suggests a chiefly ceramic origin for these elements (Table 6-11). However, Ba, Cd, Co, Cu, Ga, Hf, Mn, Mo, Nb, Ni, Sb, Sc, Sn, Th, U and Y do not show any relationship with ceramic emissions (Table 6-11). The last conclusion demonstrates that the well known relationship between some ceramic manufacture and the high levels of Hf, U and Th in atmospheric particles has a very local incidence.

Analysis of simultaneous samples of PM10 and PM2.5 shows that the crustal and marine loads are strongly reduced in PM2.5 with respect to PM10 (Table 6-12) measurements. In contrast, most of the secondary anthropogenic species are retained in the PM2.5 sampling with the exception of nitrate, which registers only 40 % of the PM10 nitrate levels. As demonstrated below,

the occurrence of calcium and sodium nitrate in the 2.5-5.0 µm range probably accounts for the lower nitrate measurements in the PM2.5 filters.

6.3.4 Cascade impactor sampling

Ammonium and ammonium-calcium sulphates are mainly concentrated in the finest fractions (0.3-0.7 and 0.7-1.0 µm, respectively). These two fine fractions account for 80 % of the bulk anthropogenic sulphate (Figure 6-37). The coarser sulphate is mostly present as calcium and sodium sulphates.

The marine aerosol phases are mainly concentrated in the 3-10 µm fraction as inferred from the Na^+ distribution (Figure 6-37). However, there is a clear grain-size segregation between the occurrence of NaCl (6-10 µm and >10 µm fractions) and the $NaNO_3$ (<6 µm fraction). This is due to the well known Na^+-NO_3^--Cl^--NH_4^+ interaction (Harrison and Pio, 1983 and Wall et al., 1988). Ammonium nitrate (originally present in the <6 µm fraction) reacts with sodium chloride to give rise to ammonium chloride (gas) and particulate sodium nitrate. The ion balance also indicates the occurrence of $Ca(NO_3)_2$ in the >6 µm fraction probably due to nitrification of soil particles (Harrison and Kito, 1990) and NH_4NO_3 in the <1.5 µm fraction (Figure 6-37).

As expected, $SO_4^=$, NO_3^-, Cl^-, NH_4^+, Ca, Mg, Mn, Pb, V and Zn have a major soluble fraction (Figure 6-37), and Al, K, Sr, Ba, Cr, Cu, Ni, Ti and Fe are mainly present in insoluble phases (Figure 6-38). Insoluble soil and ceramic particulates such as clay minerals, calcium carbonate and feldspars (crustal phases) show a bi-modal grain-size distribution with modes occurring in the 1.5-6.0 µm and >25 µm fractions as deduced from the grain-size distribution of insoluble levels of Ca, Al, K and Fe (Figure 6-38).

Soluble fractions of Mn, Fe, V and Cr, probably occurring in different oxide phases with an anthropogenic origin, are mostly in the 6 -10 µm range (Figures 4 and 5). However, Pb and Zn mainly occur in the very fine soluble fraction, >85 % of bulk Pb levels occurring in the PM2.5 fraction (Figure 6-37).

Unusually high proportions of insoluble levels of Al, Ca, Na, Sr, S, P and Fe are found in the fine grain-size modes (<1.5 µm) when compared with a normal urban or industrial grain-size distribution (Figure 6-38). This atypical occurrence of fine grain sizes for these elements and the unusually high proportion of insoluble Na levels (up to 30 % of bulk Na) are probably the result of the condensation of volatile emissions from high temperature processes developed in enamel manufacture. These peculiar patterns may be useful in tracing the input of ceramic emissions on bulk PM10 levels, since the bulk chemical patterns, characterised by high Al, Si, Fe and Ca levels, are similar to the soil end-member.

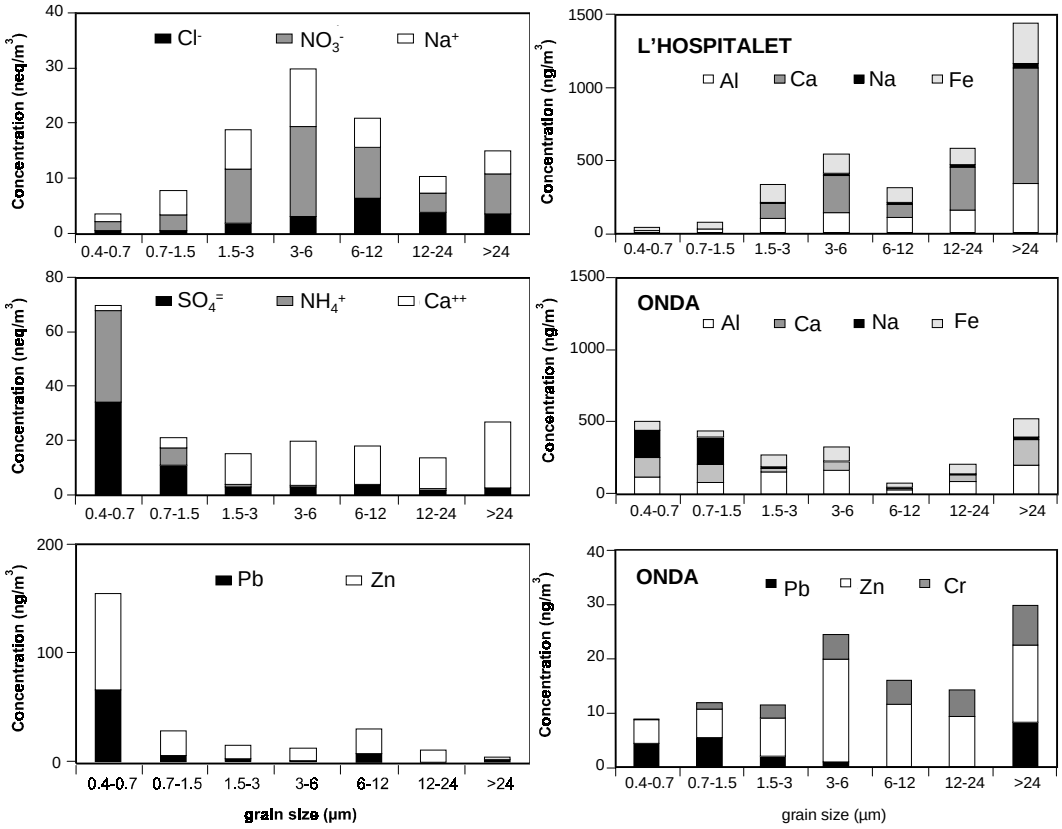

Figure 6-37

Figure 6-38

Figure 6-37. Grain-size distribution of weekly levels of the soluble fraction of major species (neq/m^3) and selected trace metals (ng/m^3) in TSP obtained at ONDA from 12-23 July 1999.
Figure 6-38. Comparison of the grain-size distributions of weekly levels of the insoluble fraction of major elements and selected trace metals in TSP obtained at ONDA with those of a typical urban distribution obtained in Barcelona. Levels in ng/m^3.

6.3.5 Grain-size distribution of PM around the emission sources

The fugitive emissions from the largest open-pit clay mine in the area induce very high ambient air PM10 levels around the mining area (approx. 300µg/m^3 were recorded on an hourly basis, Table 6-13 and Figure 6-39) but the PM2.5 fraction is relatively low (22 %wt of the PM10). The PM10 fraction also represents a low TSP fraction (40 %wt). As might be expected, this coarse grain-size distribution (high and low modes of >20 and 4-15 µm, respectively) was similar to that previously described for the clay-related elements (Al, K, Fe) obtained from the Cascade impactor sampling. The grain-size distribution of ambient air particulates around different clay atomisers and from several crossroads with high densities of clay road-based transport is also very similar (Figure 6-39 and Table 6-13), with a major proportion in the >20 µm and two secondary modes occurring in the 4-7.5 and 10-15 µm fractions. The PM10 levels around these sites also reach very high levels (from 120 to 700 µg/m^3 on an hourly basis). The percentages of PM10 over TSP and PM2.5 over PM10 are constantly low (from 30 to 45 %wt and from 40 to 45 %wt, respectively) around the four atomisers. Although the TSP grain size pattern is slightly finer around the atomisers when

Table 6-13. Levels of PM in different grain size cut off around several PM sources and in ambient air. See location in Figure 6-36.

		TSP	PM10	PM7.5	PM5	PM2.5	PM1.0	PM0.8
Ceramic emissions								
Fugitive emissions								
Clay mine	E-1	823	337	266	163	61	9	7
Transport	E-2	1770	704	560	340	185	21	15
Atomiser-ATESA	E-3	387	113	97	75	43	11	9
Atomiser-L'A	E-4	420	128	108	78	40	10	8
Atomiser-L'A2	E-4b	532	214	187	137	74	16	12
Around stack emissions								
Industrial source-1	E-5	349	251	223	159	83	21	16
Industrial source-2	E-6	127	56	49	38	22	6	5
Industrial source-3	E-7	353	170	158	157	150	126	120
Industrial source-4	E-8	78	38	35	30	24	12	11
Industrial source-5	E-9	83	44	40	38	35	24	23
Industrial source-6	E-10	135	64	59	49	33	12	10
Industrial source-7	E-11	267	84	75	68	57	22	17
Industrial source-8	E-12	483	218	188	142	84	21	16
Direct measurements of plume emissions								
Industrial source-9	E-12b	855	385	330	247	144	33	25
Industrial source-10	E-13	2485	1018	867	610	289	47	34
Traffic emissions								
Castelló-1	E-14	62	42	35	26	17	8	7
Castelló-2	E-15	47	27	26	23	19	9	8
Combustion emissions								
Petrochemical	E-16	25	22	21	19	15	7	6
Biomass	E-17	149	73	58	43	28	13	12
Marine aerosols								
Borriana	E-18	36	31	29	24	17	7	6
Millars	E-19	53	44	42	33	20	7	6
Ben Afeli-1	E-20	86	49	43	35	24	8	7
Ben Afeli-2	E-20b	31	28	27	25	19	7	6
Ambient air measurements at background sites								
Cross-section								
North-ceramic	A-1	55	35	32	28	22	12	12
Middle	A-2	39	24	23	22	21	11	10
Coastal	A-3	28	24	23	21	17	9	8
L'Alcora-1	A-4	91	46	42	33	22	8	8
L'Alcora-2	A-5	62	41	36	29	20	9	8
L'Alcora-3	A-6	66	43	37	27	16	7	6
L'Alcora-ONDA	A-7	33	24	22	18	15	8	7
Millars bridge	A-8	62	43	40	34	27	14	13
Mt. Bartolo	A-9	32	25	24	21	16	8	7

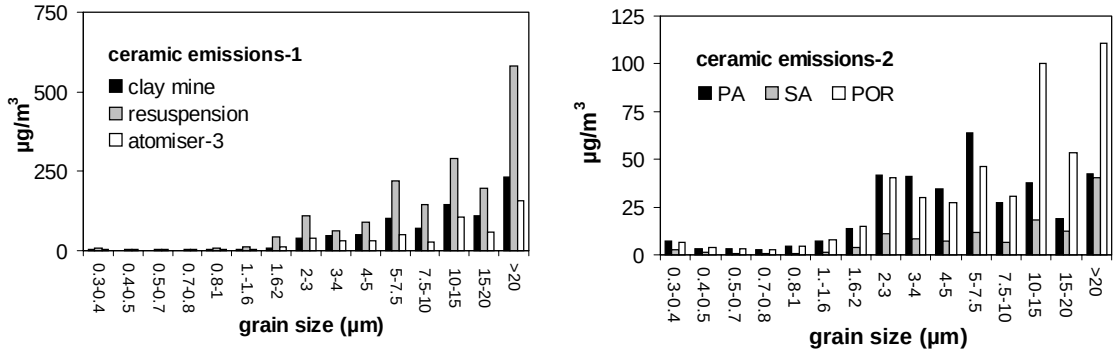

Figure 6-39. Selected cases of grain-size distribution of hourly levels of total suspended particles measured in the vicinities of the major ceramic emission sources. Levels in µg/m^3. See codes in Table 6-13 and Figure 6-36 for location of measurement sites.

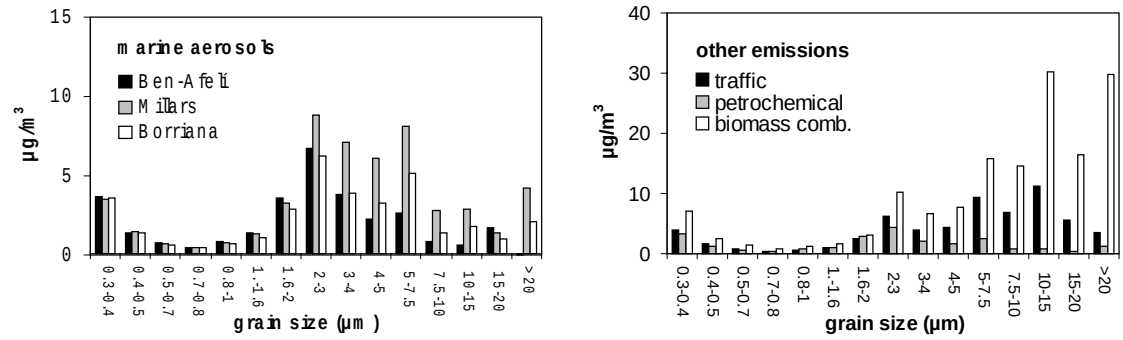

Figure 6-40. Selected cases of grain-size distribution of hourly levels of total suspended particles measured in the vicinities of non-ceramic emission sources. Levels in µg/m^3. See codes in Table 6-13 and Figure 6-36 for location of measurement sites.

compared with the fugitive emissions from clay mining and transport, the similarity of these grain-size distributions suggests that the major emission source from these activities is the fugitive emissions from the large clay stockpiles and transport.

PM10 levels are significantly lower around the 10 ceramic factories including tiling and enamel factories than around the mining, atomiser and clay-transport sources (Table 6-13 and Figure 6-39). Levels ranging from 40 to 250 µg/m^3 of PM10 on an hourly basis are obtained around these factories which emit particulate matter mainly through small-stacks. The percentage of PM10 in TSP and that of PM2.5 in PM10 increase considerably with respect to the previous emission sources. Although a similar percentage of PM10 in TSP is determined for both tiling and enamel factories (from 50 to 65 %wt), the enamel sources are characterised by a higher proportion of fine particles (from 80 to 95 %wt of PM10 are in the PM2.5 range) with respect to the tiling factories (60 to 70 %wt of PM10 are in the PM2.5 range).

The grain-size distribution of traffic particulate emissions was measured at different places in the study area including a major crossroads in the area of ceramic manufacture and in the town of Castelló. Under typical summer conditions, direct traffic emissions do not give rise to high PM10 ambient air levels. PM10 levels of 30 to 40 µg/m^3 on an hourly basis were obtained around major

crossroads inside the town of Castelló (Table 6-13). The percentage of PM10 in TSP ranges between 60 and 65 %wt, whereas the percentage of PM2.5 in PM10 ranges from 45 to 70 %wt (Figure 6-40).

Intermediate PM10 ambient air levels (around 70 μg/m^3 of PM10 for a 1/2 hour basis) are obtained in areas with intensive biomass combustion activities around large orange tree plantations. However, the high density of biomass fires could make this emission type a very important source for PM10 in the study area. In the vicinity of the fires the percentage of PM10 in TSP is approx 50 %wt, whereas the PM2.5 fraction in PM10 reaches only 40 %wt (Table 6-13 and Figure 6-40).

Measurements of the marine aerosols, obtained at different sites of the shoreline in periods with a dominant daytime in-land breeze flow, show PM10 levels from 25 to 50 μg/m^3 of PM10 (on an hourly basis). The percentage of PM10 in TSP is constantly around 85 %wt and the PM2.5 fraction in PM10 ranges from 45 to 75 %wt. Constant levels of 5 to 8 μg/m^3 are measured for fractions <0.8 μm (Table 6-13 and Figure 6-40) which coincide with the levels and the grain size distribution obtained for ammonium sulphate phases with the cascade impactor.

Measurements were also made in the plume of the petrochemical plant located on a coastal site to the south of Castelló. PM10 levels are relatively low (approx 20 μg/m^3 hourly PM10) compared with the other anthropogenic source. The grain-size distribution is very similar to the that of the marine aerosols, with levels of fine secondary particles similar to those of the background marine measurements (Figure 6-40).

6.3.6 Grain-size distribution of PM: ambient air measurements

Measurements were carried out following a cross-section from the coastal area towards the zone of ceramic production during the daytime in-land breeze circulation stage (Table 6-13). The measurements were performed in background rural and sub-urban areas. PM levels present an increasing trend from the coast (20 μgPM10/m^3 and 15 μgPM2.5/m^3) towards the areas of ceramic manufacture (36 μgPM10/m^3 and 25 μgPM2,5/m^3). The finest fraction (mainly <0.8 μm sulphate) also follows the same trend (from 8 to 12 μg/m^3). All the measurements of this cross-section also show two grain-size modes of around 1.6 to 3.0 μm and 5.0 to 7.5 μm, corresponding to marine aerosols. PM levels tend to increase in the 5.0 to 7.5 μm mode (Figure 6-41) probably because of the rise in the levels of nitrate and PM derived from primary ceramic emissions. In addition to these modes, two additional coarse particulate inputs are evident (in the 10 to 15 μm and >20 μm) as the ceramic area is approached (Figure 6-41). These grain size patterns and levels are also constantly recorded by a number of additional measurements performed at ceramic background sites around L'ALCORA and ONDA (Table 6-13 and Figure 6-41).

The results of the measurements performed at the rural background station of Mt. BARTOLO show levels of PM10 around 25 μg/m^3 from which 1/3 proceed from the ammonium sulphate phases (8 μg/m^3 in the <0.8 μm fraction). In addition to other possible particulate inputs such as nitrates and crustal particles, the two other modes (2-3 and 5-7.5 μm) identified are

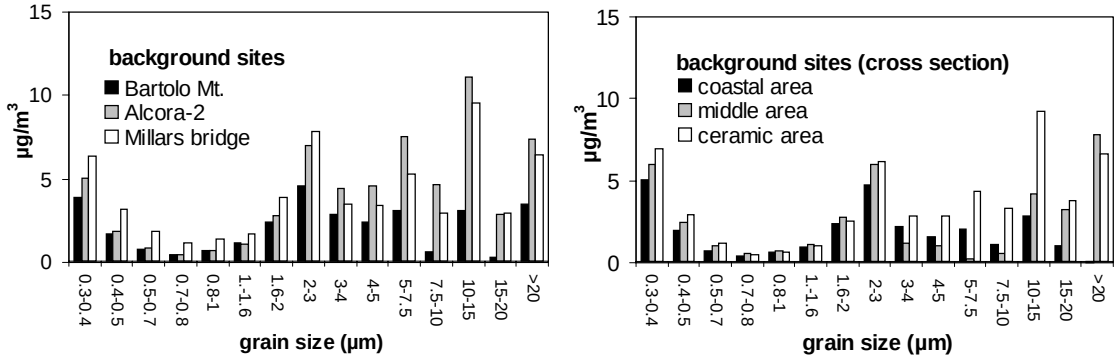

Figure 6-41. Grain-size distribution of hourly levels of total suspended particles measured in rural-remote (BARTOLO) and semi-urban (L'ALCORA and ONDA) background areas. Levels in µg/m^3. See codes in Table 6-13 and Figure 6-36 for location of measurement sites.

coincident with the bi-modal distribution of the marine aerosol (Figure 6-41). The presence of relatively high levels of ammonium sulphate at this site during the daytime breeze stage supports the high re-circulation of this secondary phase.

In summer the emission plumes from the areas of ceramic production are dragged by the nocturnal seawards breeze which leads to a rise in the night time coastal PM levels. 24-hour measurements with semi-hourly particulate levels performed at the GRAU station demonstrated that in the daytime all grain-size fractions remained at relatively low levels due to the relatively clean marine air mass flows (see levels of particles and wind velocity and direction in Figure 6-42). Later, in the nocturnal period (21 to 7 h) PM10 levels show a sharp increase as a consequence of the seaward transport of pollutants from the area of ceramic manufacture (Figure 6-42). However, levels of PM1 and PM2.5 do not exhibit major changes during the daily cycle, with the 2.5-10 µm factions being responsible for the increase in PM10 levels (Figure 6-42). Because of the longer transport of pollutants, the increase in the >10 µm fraction registered close to the ceramic emission sources (ONDA) is not recorded at the GRAU station.

The high impact of 2.5-10 µm particles on bulk PM10 levels is also evidenced by the measurements performed at L'ALCORA. At this site, high levels of PM25 and PM10 are reached during daytime, when local ceramic emissions are relatively high. In this period the emission plumes are dragged towards the northwestern areas by the inland breeze circulation. Subsequently, in the nocturnal period, these high particulate air masses travel back to the emission-source area because of the seaward breeze. These processes account for the higher PM10 levels reached at night with respect to daytime (Figure 6-42). Owing to the breeze transport and consequent grain-size segregation, nocturnal levels of >10 µm particles are low when compared with the daytime period. Once again it becomes evident that the grain-size range which detects the impact of these polluted air masses on the ambient air quality of this area is that of 2.5-10 µm (Figure 6-42). The two major PM10 peaks registered between 21-22 h and 7-8 h (both LST, see Figure 6-42) probably mark the calm periods that occur during the change in wind direction between the breeze stages.

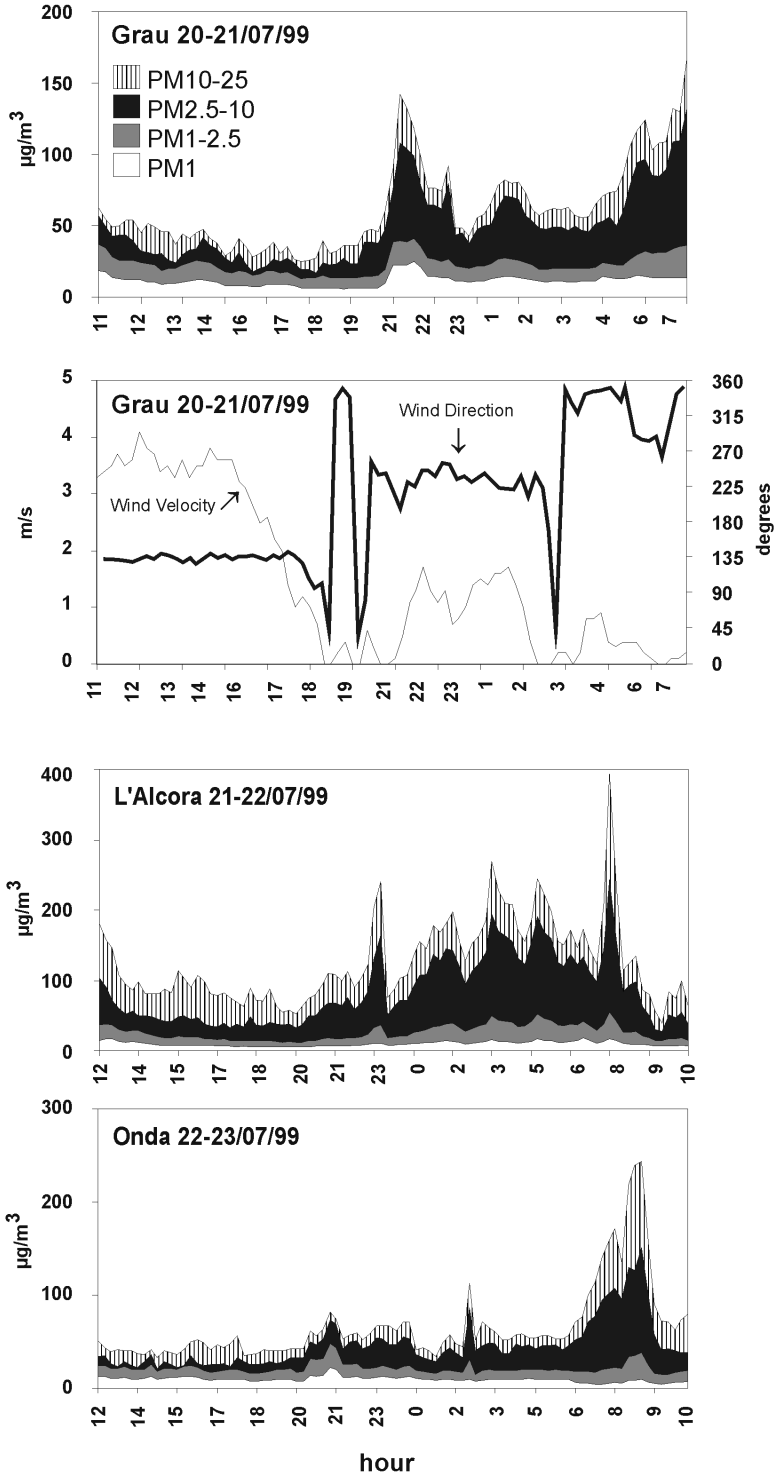

Figure 6-42. Time (LST) evolution of levels of different grain-size fractions of atmospheric particulates in the daily breeze cycle at the GRAU, ONDA and L'ALCORA monitoring stations. Levels in µg/m^3. The simultaneous wind speed and direction measurements are also included to show the breeze dynamics observed during the measuring period.

A similar situation arises at the ONDA station where the impact of emission plumes from the nearby ceramic emission sources is not as considerable as at L'ALCORA, but the nocturnal breeze circulation also accounts for high 2.5-10 and >10 µm particulate levels. The PM2.5 levels show no evidence of the impact of these plumes at all (Figure 6-42). The calm periods between breeze stages are also observed in the late evening and early morning by high particulate events (Figure 6-42).

6.4 Summary and Conclusions

Measurements of grain size distribution of PM and sampling of PM10, PM2.5 and TSP size segregated fractions in a cascade impactor were performed in an urban environment, in a rural area affected by industrial emissions of secondary particles and in an industrial area affected by primary particles emissions. The aim of the study is to assess the suitability of PM10 and PM2.5 for monitoring PM levels resulting from different types of industrial and urban emissions.

In the Barcelona Metropolitan Area, the daily traffic pattern induces a daily evolution in the grain size distribution of ambient PM. The PM2.5/PM10 ratio reaches minimum values (~0.6) during the rush hour in the morning and late afternoon, and maximum values (~0.8) at noon and at night. This daily evolution is caused by the re-suspension of coarse (2.5-10µm) road dust in the rush hour and its subsequent sedimentation. Owing to this rise in the coarse road dust levels and given the longer residence time of the fine particles, the amplitude of the daily cycle of TSP (~49µg/m^3) and PM10 (~37µg/m^3) is much higher than that of PM2.5 (~15µg/m^3) and PM1 (~13µg/m^3). Thus, the variations in PM10 levels has a higher noise than PM2.5 and PM1.

Levels of PM2.5 and PM1 undergo a seasonal evolution characterised by a winter maximum owing to the enhanced formation of particles from vehicle exhaust emissions (nitrate and organic PM). In urban environments, PM emissions derived from road traffic affect both the fine (<2.5µm) and the coarse (2.5-10µm) modes of PM. At theses sites, PM2.5 is an indicator of PM, which results from vehicle exhaust emissions, whereas the 2.5-10µm fraction is mainly constituted by road dust.

In the rural area of the Ebro basin affected by the SO_2 emissions from the Teruel power plant, the value of the PM2.5/PM10 ratio undergoes wide variations. At sites affected by the re-suspension of mineral dust because of natural causes, crop cultivation or grazing, the ratio PM2.5/PM10 is very low (down to 0.15). A higher PM2.5/PM10 ratio is found in ambient air (0.4-0.7). During fumigations of the SO_2 plume, a very high PM2.5/PM10 ratio is found (0.7-0.9). Owing to the occurrence of coarse particles in ambient air and to the fact that sulphate occurs in the fine fraction of PM, PM10 is not a suitable parameter for detecting the fumigations of the SO_2 plume. In contrast, PM1 and PM2.5 do detect the fumigations of the SO_2 plume satisfactorily.

In the area of ceramic production in Castelló, particulate emissions have a coarse grain-size distribution, resulting in low PM2.5/PM10 ratios (~0.3) around most PM sources. However, the particulate transport dominated by the breeze circulation in summer accounts for a subsequent grain-size segregation, resulting in a higher PM2.5/PM10 ratios (~ 0.6) in ambient air. Major

impacts on the ambient air quality of the coastal area induced by the particulate ceramic emissions occur in the nocturnal period due to the seawards transport of polluted air masses. Levels of ambient air particles increase mainly in the range 2.5-10 μm because of the grain-size segregation by transport.

Although the implementation of a PM2.5 standard, in addition to PM10, for ambient air quality monitoring standards is a likely trend for the future in Europe, PM2.5 is not a suitable parameter for monitoring the impact of primary particulate emissions (such as emissions from ceramics, mining, cement or concrete manufacture) on air quality since the major particulate ambient air levels are in the range 2.5-10 μm.

Based on the analysis of major and trace elements in PM10, PM2.5 and TSP size segregated fractions and on GRIMM measurements, it may be concluded that the measurements of PM2.5 significantly reduced the interference of crustal particulates without a major reduction in the secondary anthropogenic load with the exception of nitrate. However, some industrial activities result in coarse primary PM emissions and consequently PM2.5 measurements are not suitable for PM monitoring. From a technical point of view, the parameter used for PM monitoring should be selected as function of the type of anthropogenic activity. PM2.5 is a suitable parameter for PM monitoring in areas mainly affected by secondary particulate emissions. Moreover, the load of crustal particulates in PM2.5 is significantly reduced with respect to PM10. PM10 should be used in areas where primary anthropogenic particulate emissions need to be monitored.